

Original Article

Root aquaporins contribute to whole plant water fluxes under drought stress in rice (*Oryza sativa* L.)Alexandre Grondin^{1,3}, Ramil Mauleon¹, Vincent Vadez² & Amelia Henry¹¹International Rice Research Institute, Crop Environmental Sciences Division, DAPO Box 7777, Metro Manila, Philippines, ²International Crops Research Institute for the Semi-Arid Tropics, Patancheru, 502 324, Andhra Pradesh, India and ³University of Nebraska-Lincoln, Department of Agronomy and Horticulture, Lincoln, NE 68583, USA

ABSTRACT

Aquaporin activity and root anatomy may affect root hydraulic properties under drought stress. To better understand the function of aquaporins in rice root water fluxes under drought, we studied the root hydraulic conductivity (*Lpr*) and root sap exudation rate (*Sr*) in the presence or absence of an aquaporin inhibitor (azide) under well-watered conditions and following drought stress in six diverse rice varieties. Varieties varied in *Lpr* and *Sr* under both conditions. The contribution of aquaporins to *Lpr* was generally high (up to 79% under well-watered conditions and 85% under drought stress) and differentially regulated under drought. Aquaporin contribution to *Sr* increased in most varieties after drought, suggesting a crucial role for aquaporins in osmotic water fluxes during drought and recovery. Furthermore, root plasma membrane aquaporin (PIP) expression and root anatomical properties were correlated with hydraulic traits. Three chromosome regions highly correlated with hydraulic traits of the OryzaSNP panel were identified, but did not co-locate with known aquaporins. These results therefore highlight the importance of aquaporins in the rice root radial water pathway, but emphasize the complex range of additional mechanisms related to root water fluxes and drought response.

Key-words: aquaporins; plasma membrane intrinsic proteins; azide; root hydraulic conductivity; sap exudation; leaf water potential; transpiration rate.

INTRODUCTION

The root system is responsible for capturing water and nutrients and thus has been intensively studied in order to improve rice adaptation to drought stress (Gowda *et al.* 2011; Rogers & Benfey 2015). Limitations to rice root water uptake under drought have mostly been studied in terms of root architecture; more research is needed on the functionality of the root system under drought (Vadez 2014). Because of its ability to grow in flooded paddies as well as in dry soil, in large and diverse cultivation areas worldwide, rice varieties offer a potentially unique panel of variability in root water uptake

functionality and regulation that can be used for quantitative analyses (Henry *et al.* 2011; Gowda *et al.* 2012).

Rice roots tend to have lower hydraulic conductivity than other herbaceous species such as maize (*Zea mays*) or common bean (*Phaseolus vulgaris*; Fiscus 1986; Zimmermann *et al.* 2000; Miyamoto *et al.* 2001), and are not able to extract as much water from drying soil (Kamoshita *et al.* 2000; Kondo *et al.* 2000). The apoplastic barriers are exceptionally developed in rice roots and are reportedly responsible for the overall low root hydraulic conductivity (Miyamoto *et al.* 2001; Ranathunge *et al.* 2003, 2004). Apart from the apoplastic path in which water flow can be modulated by such barriers, the composite model of radial water transport in roots also predicts cell-to-cell water movement, i.e. symplastic routes through cytoplasmic continuity and transcellular paths crossing cell membranes (Steudle 2000). The transcellular path can play a major role as it is facilitated by water channel proteins, aquaporins (Javot & Maurel 2002). In rice, the contributions of the apoplastic and transcellular paths have been explored using ink as a partial apoplastic blocker or mercuric chloride as an aquaporin inhibitor, and the results suggested a relatively larger apoplastic flow in the outer part of the root cross section (Ranathunge *et al.* 2004).

Depending on the environmental conditions, plants can alter the relative contributions of the apoplastic and cell-to-cell pathways and therefore their overall root hydraulic conductivity (Javot & Maurel 2002). Suberization has been observed to be reduced at the exodermis but increased at the endodermis in rice plants grown in dry soil, suggesting reduced dependence on the apoplastic pathway at the inner part of the roots under such conditions (Henry *et al.* 2012). Furthermore, modulation of root hydraulic conductivity (*Lpr*) through aquaporin function can contribute to maintaining or adjusting transpiration and shoot growth according to water availability (Maurel *et al.* 2010). In rice seedlings, root-to-leaf conductance and shoot growth were significantly affected by mercuric chloride application under water-limited conditions, but not in well-watered conditions, suggesting predominantly apoplastic water transport under well-watered conditions and an upregulation of the transcellular path under water deficit (Lu & Neumann 1999). Additionally, a strong positive correlation between root hydraulic conductance and shoot dry weight was observed in three rice varieties under reduced soil

Correspondence: A. Henry. e-mail: a.henry@irri.org

water availability, but not under well-irrigated conditions (Matsuo *et al.* 2009). Studies of comparative responses of aquaporin expression, root water fluxes and plant water use measured at different times of day suggested that coordinated up-regulation of root aquaporin expression could prevent reduction in transpiration by increasing root water flow (Sakurai-Ishikawa *et al.* 2011; Nada & Abogadallah 2014). Altogether, these observations suggest that aquaporins are good target proteins for understanding limitations to rice water uptake and drought response.

In rice, 33 aquaporin isoforms have been identified, including about 11 plasma membrane intrinsic proteins (PIPs) which are the most abundant aquaporins at the plasma membrane, 10 tonoplast intrinsic proteins (TIPs), 10 nodulin 26-like intrinsic proteins (NIPs) and two small intrinsic proteins (SIPs; Sakurai *et al.* 2005; Guo *et al.* 2006; Nguyen *et al.* 2013). Aquaporins are present throughout the rice plant, some isoforms showing distinct cell-specific and tissue-specific localizations (Guo *et al.* 2006; Sakurai *et al.* 2008). For instance, PIP2;3 and PIP2;5, showed predominant accumulation in the endodermis (Sakurai *et al.* 2008). In rice and other species, the expression of PIPs fluctuates with the time of day, and also in response to various stresses such as salt, drought, cold and submergence (Malz & Sauter 1999; Lian *et al.* 2004; Ahamed *et al.* 2012; Henry *et al.* 2012; Liu *et al.* 2013). Expression analysis of PIPs under simulated drought conditions using PEG or after abscisic acid application showed different time- and stress severity-dependant responses among isoforms, where the mRNA level of some PIPs was significantly upregulated while others remained unchanged or were down-regulated (Guo *et al.* 2006; Lian *et al.* 2006). Interestingly, comparison of PIP expression between lowland (more susceptible to drought) and upland (typically more resistant to drought) varieties suggested different regulation mechanisms of PIP expression, with upland varieties showing specific up-regulation of PIP isoform genes (Lian *et al.* 2006).

Given the converging evidence linking aquaporin function to drought stress in rice, we hypothesized that aquaporin function would explain differences in root water uptake between varieties, and consequently resistance to drought stress. To our knowledge, the function of aquaporins in rice drought resistance has only been assessed using transgenic strategies (Katsuhara *et al.* 2003; Lian *et al.* 2004, 2006; Guo *et al.* 2006; Li *et al.* 2008), in which the beneficial effect of the aquaporin transgene expression in terms of growth or water content was described after growing the plants in hydroponic conditions with simulated drought stress. In this study, we assessed the variability of root hydraulic response to drought in soil-grown rice using a subset of six varieties from the OryzaSNP panel (Azucena, Moroberekan, FR13 A, Dular, IR64 and Swarna) showing a wide range of response to drought (Henry *et al.* 2011; Gowda *et al.* 2012), and we used the full OryzaSNP panel for genetic mapping. Our approach was to focus on aquaporin inhibition while taking into account the variation in PIP expression, root anatomy and plant water status in order to better understand rice root water fluxes and drought response.

MATERIALS AND METHODS

Plant material and growth conditions

Two groups of rice varieties were used in this study: (1) a subset of six rice varieties from the OryzaSNP panel comprising Azucena (japonica group), Dular (aus group) and Moroberekan (japonica group) that are typically considered as upland varieties with moderate drought tolerance, and FR13 A (aus group), IR64 (indica group) and Swarna (indica group) that are considered as lowland varieties with low drought tolerance; and (2) the 20 varieties of the OryzaSNP panel, which has been mapped for 160 000 SNP markers and shows a wide range of response to drought (McNally *et al.* 2009; Henry *et al.* 2011; Gowda *et al.* 2012). The subset of six rice varieties was used for detailed characterization of hydraulic properties under well-watered and drought stress conditions in Experiments 1–4 (Table 1). All 20 varieties were used to correlate hydraulic and plants water use traits with genomic regions in Experiments 5–7 (Table 1).

Six independent pot/cylinder studies were conducted to evaluate the contribution of aquaporins to rice root water fluxes, and the relationship between root aquaporin function and leaf water status (Table 1). The size of the pots/cylinders used was determined according to the objectives of the experiment: 0.785 L mylar tubes that fit inside the pressure chamber were used for root hydraulic conductivity and aquaporin expression studies; 1.5 L pots that facilitate frequent weighing were used for sap exudation and transpiration studies.

Experiments 1–5 were performed in a greenhouse at the International Rice Research Institute (IRRI), Los Baños, Philippines (14° 11'N, 121° 15'E) in pots or cylinders arranged on tables in a randomized complete block design. Experiment 6 was performed at the International Crops Research Institute for the Semi-Arid Tropics (ICRISAT), Patancheru, India (17° 30'N, 78° 16'E) in pots arranged randomly on tables in a greenhouse. Seeds were germinated in Petri-dishes for four days at 30 °C before sowing in soil. Experiments 1 and 3 were performed using 50 cm long and 5 cm diameter mylar tubes closed at the bottom with cheesecloth-like fabric to allow absorption of solution at the lower part of the soil column. Mylar tubes were filled with 0.95 kg of dried and sieved upland soil to a height of 40 cm for a bulk density of 1.2 g cm⁻³ and placed into 40 cm long, 5.5 cm diameter PVC cylinders to keep the root zone in the dark. In Experiments 2, 4 and 5, plants were grown in 1.5 L pots filled with 1 kg of soil from the IRRI upland farm (Table S1), or with black soil mixed with vermicompost in Experiment 6. Fertilizer was not added to the soil in Experiments 1–4 as no nutrient deficiencies were observed. In Experiment 5, fertilizer (14N–14P–14K) at a rate of 0.3 g kg⁻¹ was added at 20 days after sowing (das). The well-watered condition consisted of keeping the soil saturated with water, while the drought stress treatment was applied seven days after sowing through gradual dry-down by withholding water. Pots/cylinders in the drought stress treatment were weighed three times per week to monitor the dry down rate, and, if needed, water was added to maintain the soil at 30–40% of field capacity until the end of the study.

Table 1. List of experiments. das: days after sowing; *Lpr*: root hydraulic conductivity; *Lpr_Inh*: relative *Lpr* inhibition; LWP: leaf water potential; Sr: sap exudation rate; Sr_Inh: relative Sr inhibition; Tr: transpiration rate; Tr_Inh: relative Tr inhibition; CT: canopy temperature; SDW: shoot dry weight; DRI: drought response index; WW: well-watered; DS: drought stress

Experiment	Number of varieties	Number of replications	Environment	Measurements; soil moisture treatments	Plant age at measurement (das)	Average temperature (°C)
1	6	15	Greenhouse (IRRI)	<i>Lpr</i> , <i>Lpr_Inh</i> , LWP, Root anatomy; WW, DS	29	29.5
2	6	6	Greenhouse (IRRI)	Sr, Sr_Inh; WW, DS	35	32.8
3	6	3	Greenhouse (IRRI)	Sampling for root PIP expression; WW, DS	29	29.8
4	6	8	Greenhouse (IRRI)	Tr, Tr_Inh; WW, DS	28	28.3
5	20	6	Greenhouse (IRRI)	Sr, Sr_Inh; WW	35	32.8
6	20	6	Greenhouse (ICRISAT)	Tr, Tr_Inh; WW	31	30
7	20	4	Lowland field (IRRI)	Sr, CT, SDW, DRI; WW, DS	65 to 95	26.7

A field experiment (Experiment 7) was also conducted under transplanted lowland field conditions at IRRI during the 2014 dry season (January to April) in order to investigate relationships between root and leaf hydraulics and plant water use related traits. Four replications of 3.5 m² plots (6 rows of 15 hills) were arranged in a randomized complete block design. Well-watered plots were maintained flooded during the entire experiment while drought was applied and managed in stress plots by withholding irrigation at 60 das as described by Henry *et al.* (2011). Tensiometers (Soilmoisture Equipment Corp., CA, USA) were installed at a depth of 30 cm in the drought stress treatment to monitor the soil water potential (Figure S1). Ambient conditions were monitored throughout the experiment (Figure S2). Basal fertilizer was applied before transplanting using complete fertilizer (14N–14P–14K) at the rate of 40 kg N ha⁻¹, and a topdressing of 50 kg N ha⁻¹ ammonium sulfate was applied before panicle initiation. Manual weeding was done when needed.

Root hydraulic conductivity

Root hydraulic conductivity (*Lpr*) was measured according to a protocol adapted from Henry *et al.* (2012). Seeds were sown at staggered intervals (12 cylinders per day) according to the number of plants that could be measured per day for *Lpr* using two pressure chambers. In a preliminary experiment, different *Lpr* inhibition protocols were explored on plants grown in soil in a growth chamber (temperature: 29 °C day, 21 °C night; relative humidity: 70%; photoperiod: 12 h) using two aquaporin inhibitors, salt (500 mM NaCl₂) and azide (4 mM NaN₃). The efficiency of the two inhibitors was tested in solution after washing the roots or by direct application into the soil, and after two treatment times (30 or 60 min; Figure S3). Azide application into the soil for 30 min was chosen to conduct further inhibition assays. In Experiment 1, *Lpr* was measured at 29 das from 7:30 AM to 1:00 PM in a greenhouse in which a total of 150 mL of water (control) or 4 mM azide solution was added directly to the soil surface and at the bottom of the mylar tube (within the outer PVC cylinder) 30 min before excising the shoots to start the *Lpr* measurements. The mylar tube was placed in a 1.6 L pressure chamber (300HGBL Plant Water

Status Console, Soilmoisture Equipment Corp., CA, USA). The main tiller was cut at a height of about 5 cm above the soil surface and passed throughout a silicone grommet in the lid of the pressure chamber while the intact root system was sealed inside. Roots were pressurized with compressed air first at 0.2 MPa for 10 min to equilibrate, and then xylem sap was collected at pressures of 0.2, 0.35 and 0.5 MPa for 10 min using pre-weighed 2 mL Eppendorf tubes filled with cotton. The mass of xylem sap exuded at each pressure was determined by weighing the cotton-filled tubes. After the sap collections, maximum root depth of each plant was measured and roots were washed and stored in 75% ethanol until scanning at 600 dpi (Epson Perfection V700, Epo America, CA, USA). The scanned roots were analysed for total root length, surface area, and length within diameter classes using WhinRhizo Pro v. 2013e (Regent Instruments, Quebec, Canada). The proportion of lateral roots for each plant was calculated by dividing the length of roots <0.2 mm in diameter by the total root length. *Lpr* was calculated as the slope of xylem sap flux at each pressure, and normalized for root surface area. Relative *Lpr* inhibition (*Lpr_Inh*) for each azide treated plant was calculated as: ($Lpr_{\text{water}}(\text{variety mean}) - Lpr_{\text{azide}}(\text{individual replicate})$) / $Lpr_{\text{water}}(\text{variety mean}) \times 100$ (Eqn 1).

Sap exudation rate

Sap exudation rate (Sr) measurements were carried out at 35 das in Experiments 2 and 5, and at 82 das in Experiment 7, according to the protocol described by Morita & Abe (2002) and Henry *et al.* (2012). Shoots were cut at a height of around 15 cm from the soil surface, and the sap coming from the root zone was collected by covering the cut stems with a cotton towel inside a polyethylene bag sealed at the base with a rubber band. After 4 h, the previously weighed towel, plastic bag and rubber band were collected and immediately weighed again to quantify the exuded sap from the intact root system. In Experiments 2 and 5 but not in Experiment 7, 150 mL of water or azide solution at 4 mM was added to the soil just before excising the shoots to collect the sap. Shoots and roots were washed after sap collection, oven-dried and weighed to determine root biomass. Sr was

calculated as grams of sap exuded per hour, and values were normalized by root mass of the plant from which sap was collected in Experiments 2 and 5. In field Experiment 7, because root mass was not measured, Sr (Sr_{DS}) was normalized by the shoot dry weight of the hill from which sap was collected in order to account for variation in plant size. Relative Sr inhibition (Sr_{Inh}) for each azide treated plant was calculated as: $(Sr_{water} \text{ (variety mean)} - Sr_{azide} \text{ (individual replicate)}) / Sr_{water} \text{ (variety mean)} \times 100$ (Eqn 2).

Leaf water potential

Leaf water potential (LWP) was measured in Experiment 1 by inserting one leaf into a pressure chamber (300HGBL Plant Water Status Console, Soilmoisture Equipment Corp., CA, USA) and pressurizing the leaf using compressed N₂ until the first drop of sap was visible at the base of the stem, at which time the pressure was recorded. LWP was measured on one leaf before adding 150 mL of water or 4 mM azide solution to the soil, and on another leaf just before cutting the shoots to measure the Lpr 30 min after the addition of solution.

Transpiration rate under rising vapour pressure deficit

Transpiration rate (Tr) was measured in a growth chamber at 28 and 31 das in Experiments 4 and 6, respectively, according to the protocol of Kholová *et al.* (2010). Twelve hours before the measurement, plants were transferred from the greenhouse to the growth chamber for night-time acclimation (23°C and 80% relative humidity), and the soil surface around each plant was covered with a plastic bag to reduce water evaporation from the soil. On the day of measurement, each pot was weighed hourly from 8:00 AM to 4:00 PM, while the vapour pressure deficit (VPD) in the growth chamber was increased by 0.4 kPa every hour (starting from 0.6 kPa at 8:00 AM to 4.1 kPa at 4:00 PM; Table S2). After the 11:00 AM weighing, 150 mL of water or 4 mM azide solution was added directly to the soil. After the last weighing (4:00 PM), shoots were harvested and stored in a plastic bag inside an ice box, and leaf area was measured with a roller-belt-type leaf area meter (LI-3100C, Li-Cor, Nebraska, USA). Plant Tr was calculated as the cumulative water loss between 11:00 AM and 1:00 PM in grams per hour, and values were normalized by the total leaf area. Relative Tr inhibition (Tr_{Inh}) for each azide-treated plant was calculated as: $(Water_loss_{water} \text{ (variety mean)} - Water_loss_{azide} \text{ (individual replicate)}) / Water_loss_{water} \text{ (variety mean)} \times 100$ (Eqn 3).

Real-time reverse transcription-polymerase chain reaction

Roots from plants grown in Experiment 3 were sampled for PIP expression analysis from 10:00 AM to 11:00 AM at 29 das, and rinsed carefully and quickly. A 15 cm length of

root was collected from the apex of the longest nodal root and immediately placed into liquid nitrogen for grinding with a frozen mortar and pestle. Powdered root tissue (150 mg) was used for RNA extraction using an RNeasy Plant mini kit (Qiagen, Germany). Three microlitres of the extracted RNA was treated with RQ1 RNase-Free DNase (Promega, Wisconsin, USA), and first strand cDNA was synthesized using a Transcriptor First Strand cDNA Synthesis kit (Roche, Switzerland) according to the manufacturers' instructions. Real-time reverse transcription-polymerase chain reaction (RT-PCR) was performed using 1 µL of diluted RNA (1:9) with a LightCycler® 480 SYBR Green I Master in a LightCycler® 480 system (Roche, Switzerland). The reaction was repeated for 30–35 cycles at annealing temperatures of 58°C for $PIP1;3/PIP2;2/PIP2;4/PIP2;6$ primers, 60°C for $PIP2;1/PIP2;5$ primers and 64°C $PIP1;1/PIP1;2/PIP2;8$ primers. Primers used to amplify the different aquaporin isoforms (Table S3) were derived from primers designed by Sakurai *et al.* (2005). Primer efficiency was tested by DNA amplification in each variety. $PIP2;5$ was not included in the analysis because of the uncertainty in the sequence. Furthermore, non-specific amplification was observed for $PIP2;3$ and $PIP2;7$ at increased annealing temperatures in all varieties making those results not suitable for analysis.

Root anatomy

Roots from Experiment 1 were sampled after the Lpr measurement (29 das) and used to investigate root anatomical properties of the six different varieties. Three intact nodal roots from single plants were randomly selected and hand-sectioned under a dissecting microscope at 1.5 and 5 cm from the root apex. Images of four sections per location along the nodal root were acquired with a Zeiss Axioplan 2 compound microscope at 50× and 100× magnification. For each section, the 50× images were used for measuring root diameter (RD), stele diameter (SD) and cortical cell file number (CCN; Lynch 2013), while the 100× images were used for measuring metaxylem diameter (MD), in both cases using Image J. v 1.46r (Abramoff *et al.* 2004). Cortical width (CW) was calculated as RD minus SD, and cortex cell diameter (CCD) was estimated as CW divided by CCN. In each image, root cortical aerenchyma (Ae) was measured on 50× images using the magic wand tool of Gimp v. 2.8.10 (GNU Image manipulation programme) and calculated as a percentage of the root cortex area.

Plant water use related measurements in the field

Canopy temperature (CT) was measured in Experiment 7 with a hand-held data-logging infrared sensor (Apogee Instruments, Logan UT, USA) at three locations per plot throughout the drought stress treatment. Data recorded at 81 das are presented (Table S13). Time to flowering was recorded when 50% of the plants in the plot reached flowering and was expressed as das. At physiological maturity, plants from an area

of 1.5 m² per plot were harvested for shoot dry weight (SDW) and grain weight (GY) measurements expressed as g m⁻². Reduction in SDW under drought stress (DS) compared to the well-watered treatment (WW) was calculated as: $(SDW_{WW}(\text{variety mean}) - SDW_{DS}(\text{individual replicate})) / SDW_{WW}(\text{variety mean}) \times 100$ (Eqn 4). Drought response index (DRI) was calculated according to Bidinger *et al.* (1987) as: $(GYS_{act} - GYS_{pred}) / SE \text{ of } GYS_{pred}$ (Eqn 5), where GYS_{act} is the actual GY measured in the drought stress treatment, GYS_{pred} the predicted GY for stress based on the GY and DTF under well-watered treatment as determined by multiple regression ($GY_{DS} = a + (b \times GY_{WW}) + (c \times DTF_{WW})$) (Eqn 6). Regression curves were determined using SigmaPlot v. 11.0 (Systat Software, Inc.). DRI was calculated based on the following equation: $GY_{DS} = 211.5 + (0.149 \times GY_{WW}) - (2.5 \times DTF_{ww})$ with SE = 35.6 (Eqn 7).

Identification of chromosomal regions correlated with hydraulic component traits

To identify genome blocks from the OryzaSNP panel that correlate with hydraulic and drought response traits, an introgression block regression analysis was performed according to Jahn *et al.* (2011) and Wade *et al.* (2015). Traits related to plant water transport (Sr , Sr_Inh , Tr , Tr_Inh and Sr_DS) or plant water use (CT, SDW reduction and DRI) measured in Experiments 5, 6 and 7, together with traits related to water uptake previously measured on this panel including volumetric soil moisture (VSM) in the field (Henry *et al.* 2011) and total water uptake (TWU) and total water uptake per total root length (TWU/TRL) in lysimeters (Gowda *et al.* 2012), were included in the analysis (Table S13). Briefly, introgression patterns (indicate-type blocks into aus or japonica genomes, aus-type blocks within indica or japonica genomes, or japonica-type blocks within indica or aus genomes) were defined based on SNP patterns in 100 kb windows across the genome (McNally *et al.* 2009). The 11 traits were correlated with these introgression blocks by linear regression and significant correlations identified by one-way ANOVA. A subset of 177 introgressed regions correlated with these traits was selected using the significance cutoff of $p < 0.005$. These introgressions were plotted to the rice chromosome map (MSU release 6.1; (Ouyang *et al.* 2007)) using Mapchart v. 2.2 (Voorrips 2002). Gene content in those three regions based on the Nipponbare genome annotation (genome regions translated to Michigan State University rice genome annotation project release 7; Kawahara *et al.* 2013) was identified using the IRRI GSL-Galaxy tool (<http://175.41.147.71:8080>).

Statistical analyses

Statistical analyses were performed in R v. 2.15.1 (R Development Core Team, 2008) using ANOVA (*aov* script) to detect significant differences and Least Significant Difference (LSD) test to group varieties into letter classes. PCA and correlation analyses were performed using STAR v 2.0.1 (IRRI, Philippines).

RESULTS

Selection of an aquaporin inhibitor treatment

Salt and azide are among the aquaporin inhibitors frequently used in the literature to evaluate the contribution of these proteins to L_{pr} . We tested the effects of these two inhibitors on L_{pr} either (1) after washing and transferring the roots from soil to solution or (2) by direct application into the soil. In solution, root treatment by salt and azide for 30 min did not alter L_{pr} compared to treatment with water (Figure S3). After 60 min in solution, L_{pr} was reduced after salt treatment and remained unchanged after azide treatment. In soil, L_{pr} was not affected by 30 min of salt treatment but was significantly decreased after the same duration of azide treatment. For both salt and azide, roots treated in soil for 60 min showed no significant differences in L_{pr} compared to water-treated roots. Therefore, in order to keep the soil-grown root system undisturbed and minimize the duration of the inhibitor treatment, application of azide directly into the soil for 30 min was used in this study to inhibit aquaporin function.

Contribution of aquaporins to L_{pr}

To investigate the variability of aquaporin contribution to root hydrostatic water fluxes, we measured the L_{pr} under well-watered conditions and drought stress after adding 150 mL of water (control) or 4 mM azide solution directly to the soil in Experiment 1 (Table 2). Under well-watered conditions, Azucena, Moroberekan, and FR13 A showed the highest L_{pr} values (from 5 to $6 \times 10^{-8} \text{ m}^3 \text{ m}^{-2} \text{ s}^{-1} \text{ MPa}^{-1}$) while Dular, IR64 and Swarna showed the lowest L_{pr} values (around $3 \times 10^{-8} \text{ m}^3 \text{ m}^{-2} \text{ s}^{-1} \text{ MPa}^{-1}$) after water treatment. L_{pr} was significantly reduced by drought stress, except in Swarna where it remained similar to the value observed under well-watered conditions. After drought stress, Azucena, Moroberekan, FR13 A and Swarna showed the highest L_{pr} values (from 2 to $3 \times 10^{-8} \text{ m}^3 \text{ m}^{-2} \text{ s}^{-1} \text{ MPa}^{-1}$) while Dular and IR64 showed the lowest values (around $1 \times 10^{-8} \text{ m}^3 \text{ m}^{-2} \text{ s}^{-1} \text{ MPa}^{-1}$). Azide treatment consistently reduced the L_{pr} , with significant differences among varieties and soil moisture treatments. The percentage of relative L_{pr} inhibition by azide (L_{pr_Inh}), which was interpreted as the contribution of aquaporins to the L_{pr} , varied from 40% in Dular to 80% in Azucena under well-watered conditions, and from 35% in IR64 to 85% in FR13 A under drought stress. Aquaporin contribution to L_{pr} (i.e. L_{pr_Inh}) was significantly reduced by drought stress in Azucena and IR64, significantly increased by drought stress in FR13 A and Dular and not changed in Moroberekan and Swarna. Because L_{pr} is subject to diurnal variation (Sakurai-Ishikawa *et al.* 2011; Henry *et al.* 2012), we further investigated potential changes in L_{pr} over two time periods in Experiment 1. The L_{pr} measured in the early morning (7 AM to 10 AM) was generally similar to the L_{pr} measured at mid-day (10 AM to 1 PM), except in Dular and FR13 A where L_{pr} significantly increased at mid-day under drought stress conditions only (Figure S4A and B).

Table 2. Root hydraulic conductivity (L_{pr}) and inhibition by azide of selected rice varieties. Exuded xylem sap was measured after pressurizing roots from plants grown in Experiment 1 under well-watered conditions (WW) or drought stress (DS). Prior to each measurement, soil was rewatered with 150 mL of water or azide solution (4 mM) for 30 min. L_{pr_Inh} : Relative L_{pr} inhibition. Mean \pm se of $n = 12$ – 15 plants are presented. Letters indicate different significance groups in the water or azide treatments

Variety	Soil moisture	Water treatment	Azide treatment	L_{pr_Inh} %
		10^{-8} $m^3 m^{-2} s^{-1} MPa^{-1}$	10^{-8} $m^3 m^{-2} s^{-1} MPa^{-1}$	
Azucena	WW	5.95 \pm 0.9a	1.49 \pm 0.4bc	79 \pm 5ab
	DS	2.90 \pm 0.5cd	1.14 \pm 0.2cde	61 \pm 6cd
Moroberekan	WW	5.23 \pm 0.6ab	2.57 \pm 0.4a	51 \pm 7def
	DS	2.40 \pm 0.3cde	0.90 \pm 0.2cdef	63 \pm 5bcd
FR13 A	WW	6.03 \pm 0.8a	2.69 \pm 0.3a	55 \pm 4cde
	DS	3.01 \pm 0.4cd	0.44 \pm 0.1f	85 \pm 2a
Dular	WW	3.16 \pm 0.3c	1.84 \pm 0.3b	42 \pm 11ef
	DS	1.56 \pm 0.2de	0.47 \pm 0.1ef	70 \pm 3abc
IR64	WW	3.78 \pm 0.4bc	1.05 \pm 0.2cdef	72 \pm 4abc
	DS	1.12 \pm 0.2e	0.67 \pm 0.1def	35 \pm 2f
Swarna	WW	3.28 \pm 0.6c	1.40 \pm 0.6bcd	57 \pm 9cde
	DS	3.04 \pm 0.3cd	0.94 \pm 0.1cdef	69 \pm 4abc

Similarly, the contribution of aquaporins to L_{pr} (i.e. L_{pr_Inh}) was generally maintained between early and mid-day (Figure S4C and D), except in FR13 A, where L_{pr_Inh} was significantly reduced at mid-day (Figure S4C).

Contribution of aquaporins to Sr

To estimate the variability of aquaporin contribution to osmotic water fluxes, we measured S_r under well-watered conditions and drought stress after treating the plants with 150 mL of water (control) or 4 mM azide in Experiment 2 (Table 3). Under well-watered conditions, Azucena, Moroberekan and Dular showed the highest S_r values (0.3 $g_{sap} h^{-1} g_{root}^{-1}$), and FR13 A, Dular, IR64 and Swarna showed the lowest S_r values (0.14 to 0.19 $g_{sap} h^{-1} g_{root}^{-1}$) after water treatment. Under drought stress, the absolute amount of exuded sap and the root dry weight was markedly lower

compared to the well-watered conditions (data not shown), but after normalization for root dry weight, S_r was higher under drought in all varieties, with Azucena, Moroberekan, FR13 A, Dular and Swarna showing the highest values (0.4 to 0.5 $g_{sap} h^{-1} g_{root}^{-1}$) and IR64 showing the lowest value (0.3 $g_{sap} h^{-1} g_{root}^{-1}$). After azide treatment, S_r was systematically reduced until being almost completely eliminated in Azucena under drought stress. Furthermore, significant differences in relative S_r inhibition (S_r_Inh , i.e. the contribution of aquaporins to S_r) were observed between soil moisture treatments, with Azucena and Dular displaying contrasting behaviour; Azucena showed the lowest S_r_Inh under well-watered conditions but the highest under drought stress, and Dular showed the highest S_r_Inh under well-watered conditions but the lowest under drought stress. The contribution of aquaporins to S_r was significantly increased by drought stress in Azucena,

Table 3. Sap exudation rate (S_r) and inhibition by azide of selected rice varieties. Xylem sap was collected for 4 h from roots of plants grown in Experiment 2 under well-watered conditions (WW) or drought stress (DS). Prior to the measurement, soil was rewatered with 150 mL of water or azide solution (4 mM) for 30 min. S_r_Inh : Relative S_r inhibition. Mean \pm se of $n = 3$ – 6 are presented. Letters indicate different significance groups in the water or azide treatments

Variety	Soil moisture	Water treatment	Azide treatment	S_r_Inh %
		$g_{sap} h^{-1} g_{root}^{-1}$	$g_{sap} h^{-1} g_{root}^{-1}$	
Azucena	WW	0.30 \pm 0.01bc	0.22 \pm 0.01a	27 \pm 2g
	DS	0.44 \pm 0.04a	0.01 \pm 0.01e	97 \pm 1a
Moroberekan	WW	0.30 \pm 0.05bc	0.21 \pm 0.03ab	39 \pm 4efg
	DS	0.50 \pm 0.00a	0.15 \pm 0.06abcd	69 \pm 13bcd
FR13 A	WW	0.18 \pm 0.01de	0.12 \pm 0.01cd	35 \pm 6fg
	DS	0.40 \pm 0.02ab	0.19 \pm 0.01abc	53 \pm 3def
Dular	WW	0.23 \pm 0.04cd	0.06 \pm 0.00de	73 \pm 1bc
	DS	0.43 \pm 0.08a	0.25 \pm 0.07a	40 \pm 12efg
IR64	WW	0.14 \pm 0.02e	0.06 \pm 0.00de	56 \pm 1cde
	DS	0.30 \pm 0.04bc	0.07 \pm 0.04de	86 \pm 11ab
Swarna	WW	0.19 \pm 0.02de	0.13 \pm 0.01bcd	29 \pm 7g
	DS	0.45 \pm 0.04a	0.23 \pm 0.01a	48 \pm 3ef

Moroberekan, FR13 A, IR64 and Swarna, and significantly decreased by drought stress in Dular.

Aquaporin expression profiles under well-watered and drought stress conditions

To investigate the variability of PIP expression in the roots of the six selected varieties, we measured the transcript abundance of 10 rice PIP genes (*PIP1;1*, *PIP1;2*, *PIP1;3*, *PIP2;1*, *PIP2;2*, *PIP2;3*, *PIP2;4*, *PIP2;6*, *PIP2;7* and *PIP2;8*) under well-watered and drought stress conditions using RT-PCR in Experiment 3. *PIP2;4* was not detected in Azucena or Moroberekan at the DNA and RNA level by the designed primers. Except for *PIP2;3* and *PIP2;7*, unique melting curves combined with single amplification fragments of the expected size were observed in all varieties after RT-PCR indicating PIP isoform specific amplification (Figure S5). Under well-watered conditions, significant

variation in PIP relative transcript abundance was observed among varieties ($p < 0.001$ for *PIP1;1*, *PIP1;2* and *PIP2;1*; $p < 0.01$ for *PIP1;3*, *PIP2;2* and *PIP2;6*; $p < 0.05$ for *PIP2;4* and $p < 0.01$ for *PIP2;8*; Fig. 1a). Overall, IR64 showed relatively low PIP transcript abundance compared to the other varieties while Moroberekan showed the highest relative transcript abundance of *PIP1;1*, *PIP1;2*, *PIP2;2*, *PIP2;6* and *PIP2;8* among the selected varieties and no transcript for *PIP2;1*. Under drought stress, the variation in PIP relative transcript abundance among varieties was less, although it was significant for *PIP2;1* ($p < 0.001$), *PIP1;3* and *PIP2;2* ($p < 0.01$), and *PIP1;1*, *PIP1;2* and *PIP2;8* ($p < 0.05$; Fig. 1b). In general, Swarna showed the highest level of transcript abundance for most of the PIP isoforms under drought stress, especially for *PIP1;3*.

The effect of drought stress on PIP expression was also investigated by calculating the relative expression of each PIP under drought as the fold-level increase compared to its expression under well-watered conditions for each variety

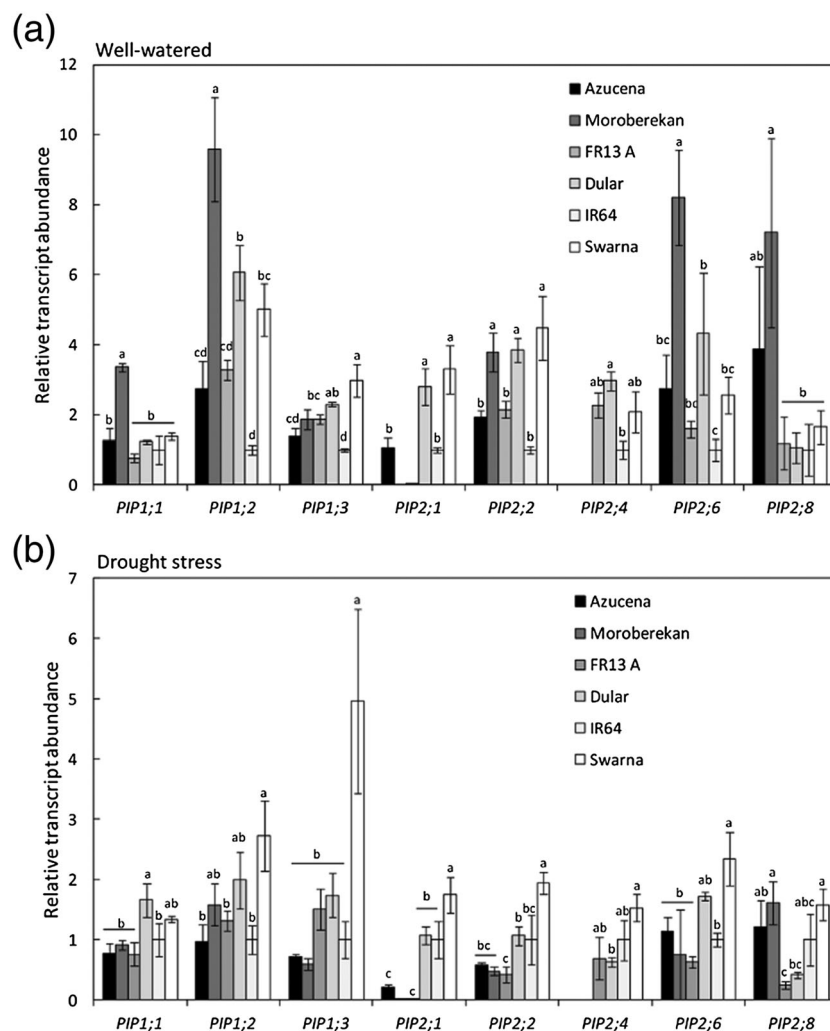


Figure 1. Relative transcript abundance of eight PIP genes in six selected rice varieties. RNA was extracted from roots grown under well-watered conditions (a) or drought stress (b) during Experiment 3. Transcript abundance of the indicated PIP gene was measured in each variety and soil moisture by RT-PCR and normalized to the expression of the same gene in IR64. Bars show mean values \pm se of $n = 3$ biological replicates, each with triplicate RT-PCR. Letters indicate different significance groups for transcript abundance of one particular PIP gene.

(Fig. 2). In general, PIP transcript accumulation was reduced (*PIP2;8*) or slightly induced (*PIP1;1*) by drought stress, although some exceptions were observed. For instance, *PIP1;2* and *PIP2;2* were particularly induced in IR64, as well as *PIP2;6* and *PIP2;8* in IR64 and Swarna.

Covariation of hydraulic properties and PIP expression

In order to better understand the relationships between PIP expression and root hydraulic traits, we performed principal component analysis (PCA) of the PIP transcript abundance, *Lpr*, *Lpr* inhibition (*Lpr_Inh*), *Sr* and *Sr* inhibition (*Sr_Inh*) measured in the six selected varieties. Under well-watered conditions, the first principal component (PC1), which accounted for 61.91% of the variability, was positive for the *Lpr* components but negative for *Sr* components and aquaporin transcript abundance (Fig. 3a). The second principal component explained 21.65% of the variability and was positive for *PIP1;1*, *PIP1;3*, *PIP2;1*, *PIP2;2* and *PIP2;8*, but negative for *PIP1;2*, *PIP2;4* and *PIP2;6* as well as *Lpr* and *Sr* components. Overall, the PCA analysis suggested negative correlations of *Lpr* and *Lpr_inh* with several PIP isoforms, and covariation of *Sr* with *PIP2;6* and *PIP2;4*. Pearson's correlation test confirmed a weak negative correlation between the transcript abundance of a number of PIPs and the *Lpr* and *Lpr_Inh* under well-watered conditions (Table S4). Positive correlations were also observed between *Sr* and *PIP2;4* ($p < 0.05$), *PIP2;6* ($p = 0.0992$) and *PIP2;8* ($p < 0.05$). Under drought stress, PCA analysis indicated little variation among varieties for PIP transcript abundance, all showing positive PC1 values, and negative or low positive PC2 values (Fig. 3b). No clear correlation profile was observed between *Lpr*, *Lpr_Inh*, *Sr*, *Sr_Inh* and PIP transcript abundance by Pearson's correlation analysis (Table S5). However, significant positive correlations among the transcript abundance of several PIP isoforms were observed under drought stress as well as under well-watered conditions (Tables S4 and S5).

PCA analysis of the effect of drought on PIP expression with *Lpr* and *Sr* components revealed a principal component explaining 62.59% of the variability that was positive for most PIP isoforms, *Lpr* *Lpr_Inh* and *Sr*, and negative for *PIP1;1* and *Sr_Inh* (Fig. 4). Covariation of all PIP relative expression levels with *Lpr* and *Sr* was also revealed (Table S6). Indeed, except for *PIP1;1*, positive correlations were observed between PIP relative expression, *Lpr* and *Sr*, with significance between *PIP2;6* and *Sr* ($p < 0.05$).

Root architecture and anatomy

Because root architecture and anatomy can strongly affect root water fluxes, we investigated the variations of these two parameters in the selected varieties in Experiments 1 and 2. Significant differences in maximum root depth were observed among varieties ($p < 0.001$), with Moroberekan showing the highest value and Swarna the lowest value under both well-watered conditions and drought stress (Table S7). Significant differences among varieties were also observed in total root length ($p < 0.001$), root surface area ($p < 0.001$) under both conditions and percentage of fine roots ($p < 0.001$) under drought stress. No significant differences were observed in root mass and root:shoot ratio. Except for the maximum root depth and the percentage of fine roots, root architecture parameters and the root:shoot ratio were reduced by drought stress.

Root anatomy was investigated in cross sections of nodal roots taken at 1.5 and 5 cm from the root apex (Table 4, Figs. 5 and S6). Azucena, Moroberekan, FR13 A and Dular had larger root diameter (RD) than FR13 A, IR64 and Swarna under well-watered conditions at both locations of the apex. Root diameter was significantly reduced by drought in all varieties, but the reduction was less marked in Moroberekan. In general, varieties with larger RD under well-watered conditions and drought stress also showed larger cortical width (CW; data not shown), stele diameter (SD), and metaxylem diameter (MD). This trend was confirmed by significant positive correlation between RD and

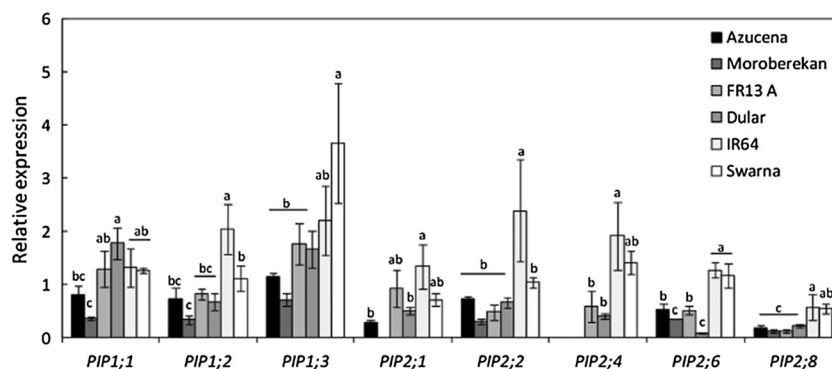


Figure 2. Variation of PIP relative expression in response to drought in six selected rice varieties. The relative transcript abundance of a particular PIP under drought was calculated in one variety as the fold increase relative to the transcript abundance in the same variety under well-watered conditions. Bars show mean values \pm se of $n = 3$ biological replicates, each with triplicate RT-PCR. Letters indicate different significance groups for transcript abundance variation of one particular PIP gene.

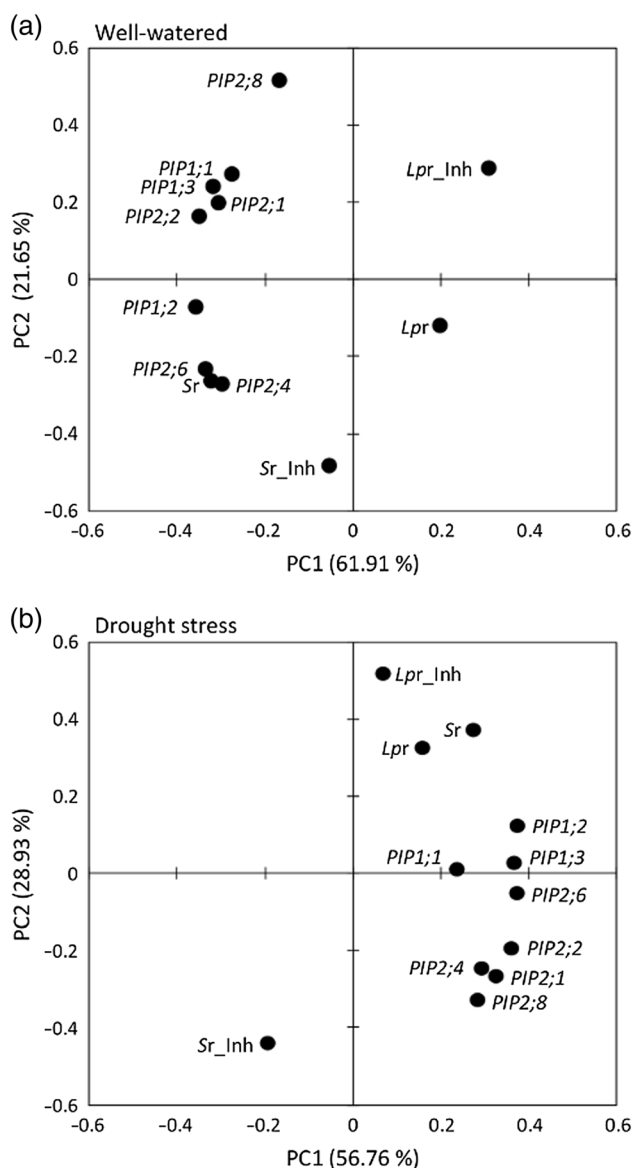


Figure 3. Covariation of root hydraulics and PIP expression in six selected rice varieties. Mean values of PIP transcript abundance, and *Lpr*, *Lpr_Inh*, *Sr* and *Sr_Inh* obtained after water treatment of well-watered (a) and drought-stressed (b) plants were used for Principal Component Analysis (PCA). The contribution of each PCA axis (PC1 and PC2) is indicated on the graph.

SD ($p < 0.05$), and RD and MD ($p < 0.05$) under well-watered conditions and drought stress at both sectioning locations (Tables S8–S11). The variability in cortical cell diameter (CCD) among varieties and soil moisture treatments was low at both sectioning locations ($p = 0.12$ at 1.5 cm and $p = 0.137$ at 5 cm; Table 4), and no correlations among CCD, RD, SD and MD were observed (Tables S8–S11). At 1.5 cm, the aerenchyma formation (Ae) varied among varieties ($p < 0.01$) and was higher in roots grown under drought stress compared to roots grown under well-watered conditions at 1.5 cm (Table 4). At 5 cm, no significant differences in Ae were observed among varieties and between soil moisture treatments ($p = 0.567$).

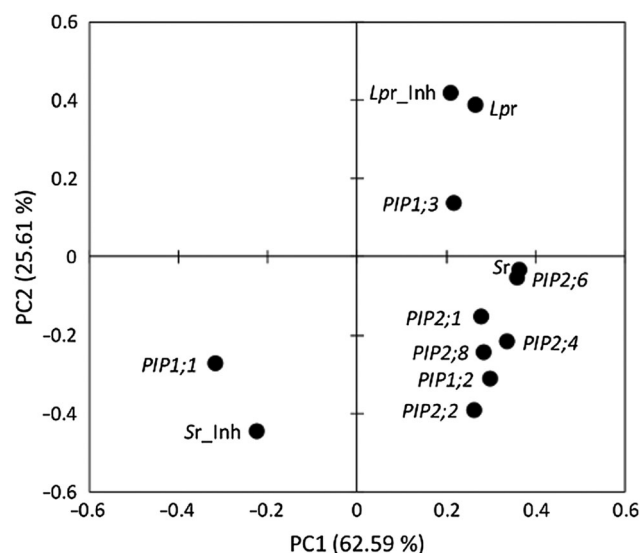


Figure 4. Covariation of root hydraulics and PIP variation in response to drought in the selected varieties. Mean values of variation of PIPs transcript abundance, *Lpr*, *Lpr_Inh*, *Sr* and *Sr_Inh* obtained after water treatment of drought-stressed plants were used for Principal Component Analysis (PCA). The contribution of each PCA axis (PC1 and PC2) is indicated on the graph.

Correlation analyses were also performed among *Lpr*, *Lpr_Inh*, *Sr*, *Sr_Inh* and all measured root anatomical parameters in order to better understand the relationship between root anatomy and root hydraulics. The analysis revealed that *Sr* was significantly positively correlated with SD ($p < 0.05$) and MD ($p < 0.05$) under well-watered conditions at both distances from the root apex (Tables S8 and S10). Under drought stress, the correlation between the stele characteristics and *Sr* remained positive but became less evident, with significant correlations only between *Sr* and MD at 1.5 cm ($p < 0.05$; Tables S9 and S11). This analysis also revealed significant positive correlations between *Lpr* and the percentage of cortical aerenchyma ($p < 0.05$) under well-watered conditions at 1.5 cm only (Table S8). No clear correlations were observed between hydraulic properties and visual observations of suberization profiles under both well-watered and drought stress.

Effect of root aquaporin inhibition on LWP and Tr

To investigate if root aquaporin function can impact leaf hydraulics in rice, we measured the LWP of well-watered and drought stressed plants before and after treatments with 150 mL of water or 4 mM azide for 30 min in Experiment 1. Under well-watered conditions, the LWP measured after water or azide treatment was similar to the LWP measured before treatment in Azucena, Moroberekan and Swarna (Fig. 6a). In FR13 A, Dular and IR64, treatment with water or azide induced an increase (less negative) of LWP in the well-watered plants, which was less marked after azide treatment in FR13 A and IR64 compared to that induced by water. Under drought stress, LWP was significantly increased (less negative) in all varieties after water treatment, whereas the recovery in LWP after azide

Table 4. Root anatomical traits of selected rice varieties. Nodal roots from Experiment 1 were sampled, washed and hand-sectioned at 1.5 cm and 5 cm from the root apex for imaging. Images were used for measuring root diameter (RD), cortical cell diameter (CCD), cortical cell diameter (CCD), percentage of cortical aerenchyma (Ae), stele diameter (SD) and metaxylem diameter (MD) per nodal root segment and per variety. Letters indicate different significance groups at each distance from the root apex

Variety	Soil moisture		RD		CCD		Ae		SD		MD	
			μm		μm		%		μm		μm	
	1.5 cm	5 cm	1.5 cm	5 cm	1.5 cm	5 cm	1.5 cm	5 cm	1.5 cm	5 cm	1.5 cm	5 cm
Azucena	WW	1090 ± 35a	1059 ± 27a	80 ± 2abc	116 ± 16abc	7 ± 3efg	40 ± 7ab	271 ± 14a	268 ± 5ab	53 ± 1a	57 ± 1a	
	DS	608 ± 109def	733 ± 107c	98 ± 41abc	68 ± 1c	33 ± 6a	38 ± 4ab	196 ± 30bcd	236 ± 22bcd	38 ± 3cd	43 ± 0.2bcde	
Moroberekan	WW	986 ± 122a	953 ± 108ab	64 ± 3c	87 ± 8bc	4 ± 0.4fg	33 ± 2ab	249 ± 35ab	250 ± 32bc	51 ± 7ab	51 ± 5ab	
	DS	760 ± 90bcd	848 ± 18bc	77 ± 12bc	93 ± 10bc	28 ± 8ab	35 ± 2ab	269 ± 43a	315 ± 40a	41 ± 5bc	50 ± 5abc	
FR13 A	WW	922 ± 44ab	993 ± 46ab	83 ± 7abc	97 ± 6bc	12 ± 2def	37 ± 5ab	194 ± 8bcd	212 ± 14bcde	38 ± 1cd	42 ± 1cde	
	DS	677 ± 81cde	691 ± 59c	79 ± 11bc	165 ± 41a	14 ± 2cde	32 ± 4ab	179 ± 19cd	196 ± 5cde	34 ± 3cd	35 ± 1ef	
Dular	WW	1020 ± 47a	1012 ± 43ab	76 ± 5bc	107 ± 14abc	2 ± 1g	37 ± 7ab	229 ± 5abc	224 ± 8bcd	41 ± 1c	44 ± 2bcd	
	DS	646 ± 49def	648 ± 71cd	118 ± 2a	92 ± 14bc	26 ± 1ab	45 ± 1a	191 ± 13bcd	198 ± 24cde	38 ± 3cd	42 ± 6cde	
IR64	WW	901 ± 78abc	853 ± 23bc	71 ± 4bc	78 ± 1bc	1 ± 0g	30 ± 1ab	177 ± 13cd	176 ± 8def	39 ± 3cd	40 ± 1cdef	
	DS	455 ± 57f	511 ± 65d	98 ± 17ab	152 ± 33ab	19 ± 3bcd	30 ± 3ab	143 ± 12d	157 ± 9ef	30 ± 1d	35 ± 2ef	
Swarna	WW	776 ± 14bcd	777 ± 7c	74 ± 4bc	90 ± 16bc	3 ± 2fg	29 ± 4b	163 ± 4d	164 ± 3ef	34 ± 1cd	38 ± 1def	
	DS	508 ± 72ef	472 ± 82d	113 ± 15a	147 ± 37ab	24 ± 2abc	32 ± 5ab	140 ± 21d	132 ± 21f	33 ± 5cd	32 ± 3f	

treatment under drought was partly or completely eliminated in FR13 A, Dular, IR64, Swarna and Azucena (Fig. 6b). By contrast, azide treatment did not affect the recovery of LWP after drought stress in Moroberekan.

Using a similar approach, we investigated the effects of root aquaporin inhibition on transpiration 2 h after treating well-watered and drought-stressed plants with 150 mL of water or 4 mM azide solution in Experiment 4 (Table 5). Under well-watered conditions, around 2-fold variation in Tr was observed among varieties with $2.99 \pm 0.40 \text{ g}_{\text{water}} \text{ h}^{-1} \text{ cm}_{\text{leaf}}^{-2}$ in IR64 and $6.19 \pm 0.51 \text{ g}_{\text{water}} \text{ h}^{-1} \text{ cm}_{\text{leaf}}^{-2}$ in Azucena after water treatment. Compared to the well-watered conditions, Tr under drought stress was significantly reduced by 1.3 to 1.9-fold in Moroberekan, IR64, Dular and Azucena, and remained similar in FR13 A and Swarna. Azide treatment to well-watered plants induced no or low Tr inhibition (Tr_{Inh}) in FR13 A and Moroberekan, and moderate Tr_{Inh} (24 to 39%) in Azucena, Dular, IR64 and Swarna with little significant differences among varieties because of the variability in the measurement. Drought stress did not induce significant changes in Tr_{inh} compared to the well-watered conditions, except in Moroberekan and FR13 A where it was significantly increased.

Pearson's correlation test was performed using values of Lpr , Lpr_{Inh} , Sr , Sr_{Inh} , LWP, Tr and Tr_{Inh} obtained after water treatment under well-watered and drought stress conditions (Table S12). Under well-watered conditions, Lpr was negatively but non-significantly correlated with Tr_{Inh} ($p = 0.0885$; Fig. 7a), whereas under drought stress the correlation between these two parameters was positive and significant (Fig. 7b; $p < 0.05$). Non-significant positive correlations were also observed between Sr and Tr_{inh} ($p = 0.0951$), and Sr and LWP ($p = 0.0937$) under drought stress (Table S12).

Chromosomal regions correlated with hydraulics and plant water use related traits

To correlate hydraulic traits with genomic regions, Experiments 5 and 6 were conducted using the 20 varieties of the OryzaSNP panel in which Sr and Tr were measured under well-watered conditions in the presence of water or azide (Table S13). Significant differences in Sr and Tr values were observed after water or azide treatments ($p < 0.001$ in both cases). Sr_{Inh} showed significant variation among varieties ($p < 0.05$), while Tr_{Inh} values showed that Tr was either increased (negative values) or inhibited (positive values) by azide application, although non significantly ($p = 0.058$). After water treatment, positive correlations were observed between Sr and Sr_{Inh} ($p < 0.05$; Figure S7A), and between Tr and Tr_{Inh} , respectively ($p < 0.01$; Figure S7B). Furthermore, to determine if genetic regions correlated with hydraulic traits would align with plant water use related traits, Experiment 7 was conducted in field conditions, where significant differences among varieties were measured for Sr_{DS} ($p < 0.01$), canopy temperature (CT; $p < 0.001$) and shoot dry weight reduction (SDW reduction; $p < 0.001$). Large variation in drought response index

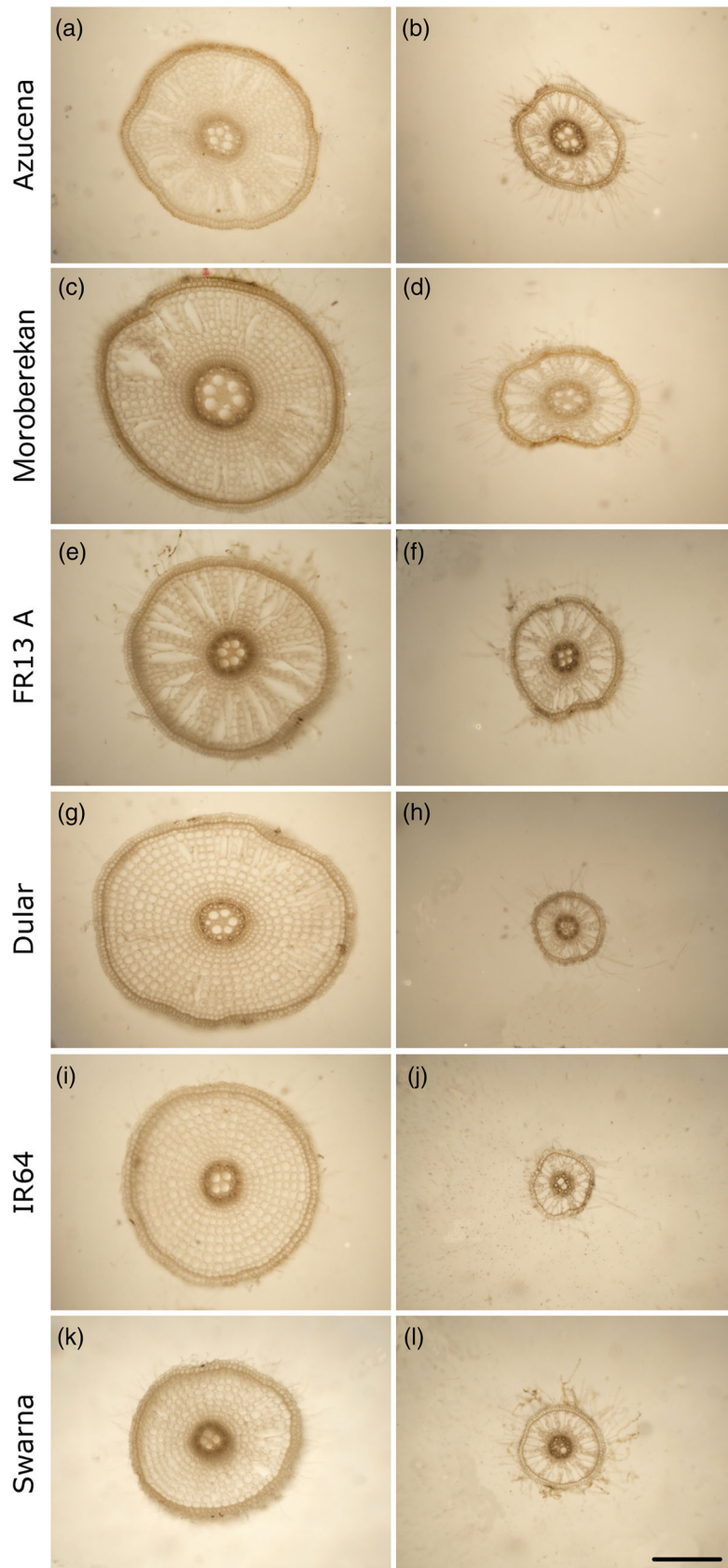


Figure 5. Root anatomy of Azucena, Moroberekan, FR13 A, Dular, IR64 and Swarna. Representative images from cross sections of nodal roots at 1.5 cm from the root apex of plants grown under well-watered conditions (a, c, e, g, i and k and drought stress (b, d, f, h, j and l) in Experiment 1 are shown. The bar represents 400 μ m.

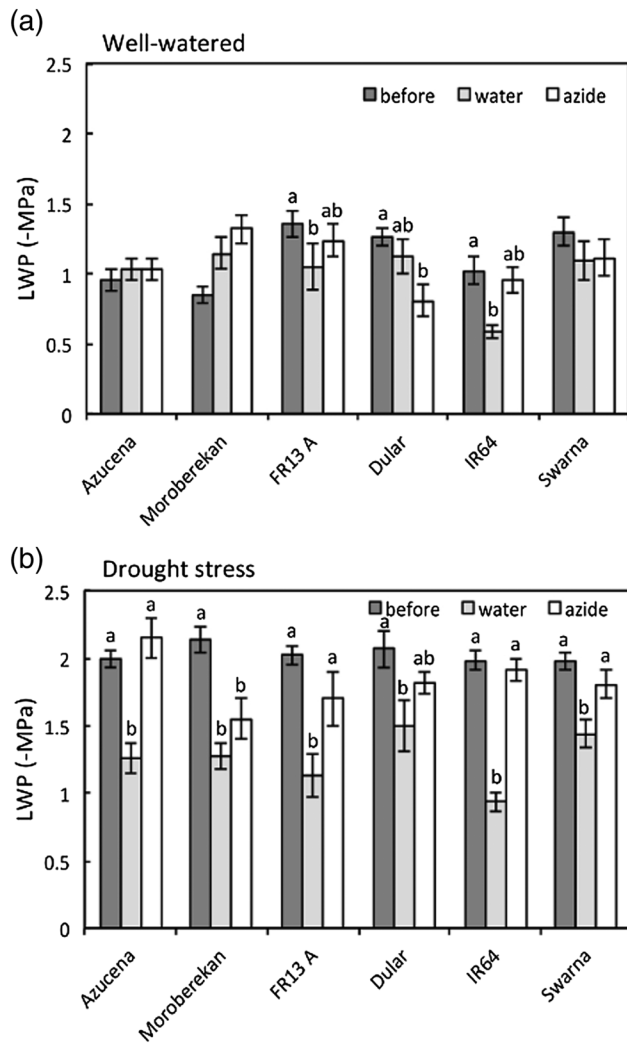


Figure 6. Effect of *Lpr* inhibition on leaf water potential (LWP) in six selected rice varieties. LWP was measured in Experiment 1 on leaves grown under well-watered conditions (a) or drought stress (b). Measurements were performed before and after treatment with water or azide solution (4 mM) for 30 min. Bars represent mean values \pm se of $n = 30$ (before) or $n = 15$ (water, azide) replicates. Letters indicate different significance groups between treatments for a particular variety.

(DRI) with values from -0.94 in Swarna to 1.81 in Dular were also observed.

Introgression block regression analysis of data from Experiments 5, 6 and 7, along with published data of water uptake on the 20 *Oryza*SNP varieties reported by Gowda *et al.* (2012) and Henry *et al.* (2011), resulted in identification of 177 significantly correlated genome regions. To further increase the confidence level of the introgressions, three regions where introgression for at least three different traits overlapped were selected (Fig. 8a); (1) region 1 on chromosome 1 (Chr01) from 8.6 to 9.3 Mb with introgressed segments correlated with *Sr_Inh* (indica-type), *Tr* (indica-type) and *CT* (aus-type); (2) region 2 on chromosome 6 (Chr06) from 5.8 to 7.9 Mb with introgressed segments correlated with *Sr_Inh* (aus-type), *TWU* (aus-type) and *CT* (aus-type); (3) region 3 on chromosome 12 (Chr12)

from 12.4 to 14.5 Mb with introgressed segments correlated with *VSM* (japonica-type), *Tr* (aus-type), *TWU/TRL* (aus-type) and *Sr_Inh* (aus-type). Gene annotation in these regions (based on the Nipponbare reference genome) showed that region 1 and 2 are relatively rich in expressed proteins (76% and 78% of the total number of genes, respectively), while region 3 is mostly composed of retrotransposons and transposons (58% of the total; Fig. 8b). No aquaporin genes were annotated in these regions, except in region 2 where a silicon influx transporter belonging to the Nodulin-26 like aquaporin subfamily (*Lsi6/NIP2-2*; Os06g0228200) was identified.

DISCUSSION

Based on the high degree of aquaporin inhibition observed, this study suggests that aquaporins can largely contribute to rice root hydrostatic and osmotic water fluxes under well-watered conditions, under drought stress and during the recovery of whole-plant water fluxes following drought stress. The analysis of PIP expression in rice roots highlights the possible role of specific PIPs in these processes, such as PIP2;4, PIP2;6 or PIP2;8. Structural parameters of rice roots such as cortical aerenchyma and stele diameter were also observed to affect root water fluxes.

Contribution of aquaporins to rice root hydraulics

We observed substantial variation in *Lpr* (1.9-fold under well-watered conditions and 2.7-fold drought stress) and *Sr* (2.1-fold under well-watered conditions and 1.6-fold under drought stress) among rice varieties, which could be respectively inhibited up to 85% in FR13 A and 97% in Azucena under drought stress. Because the percentage of inhibition of *Lpr* or *Sr* by azide can be interpreted as a reflection of the contribution of aquaporins to these processes, these results indicate that aquaporins are functional and can contribute to root water fluxes under well-watered conditions and drought stress in some rice varieties. The larger contribution of apoplastic water flow compared to aquaporin-dependent water flow that was previously reported (Ranathunge *et al.* 2004) may be a consequence of different aquaporin functional roles predominating at different parts of the root radial cross-section. This assumption is supported by the higher level of accumulation of some PIPs in the endodermis compared to other root cells (Sakurai *et al.* 2008). However, although aquaporins showed an important role in rice root function, *Tr* was not or only slightly affected by azide application under well-watered conditions and upon re-watering after a period of drought. This suggests that the aquaporin-dependent path can contribute but is not limiting to root hydrostatic water fluxes, and confirms that the apoplastic path is dominant under these conditions (Steudle 2000).

Because osmotic gradients within the roots can determine their exudation capacity (Javot & Maurel 2002), the sap exudation rate (*Sr*; also termed 'bleeding rate') can be considered as a result of osmotically driven water fluxes that involve the transcellular water pathway. The systematic

Table 5. Transpiration rate (T_r) and inhibition by azide of selected rice varieties. Transpiration rate was calculated in Experiment 4 as the cumulative water loss 2 h after rewatering plants grown under well-watered conditions (WW) or drought stress (DS) with water or azide solution (4 mM). T_r _Inh: Relative T_r inhibition. Mean \pm se of $n = 5$ –8 plants are presented. Letters indicate different significance groups in the water or azide treatments

Variety	Soil moisture	Water treatment	Azide treatment	T_r _Inh %
		10^{-2} $\text{g}_{\text{water}} \text{h}^{-1} \text{cm}^{-2}_{\text{leaf}}$	10^{-2} $\text{g}_{\text{water}} \text{h}^{-1} \text{cm}^{-2}_{\text{leaf}}$	
Azucena	WW	6.19 \pm 0.51a	4.69 \pm 0.58a	24 \pm 9abc
	DS	3.24 \pm 0.25ef	2.26 \pm 0.24d	30 \pm 7a
Moroberekan	WW	4.54 \pm 0.39bcd	4.41 \pm 0.49ab	3 \pm 11bc
	DS	3.34 \pm 0.47ef	2.17 \pm 0.13d	35 \pm 4a
FR13 A	WW	4.11 \pm 0.52cdef	4.20 \pm 0.65ab	–2 \pm 16c
	DS	4.26 \pm 0.30cde	2.69 \pm 0.24cd	37 \pm 6a
Dular	WW	5.65 \pm 0.65ab	3.46 \pm 0.63bcd	39 \pm 11a
	DS	3.51 \pm 0.38def	2.35 \pm 0.22cd	28 \pm 5ab
IR64	WW	4.65 \pm 0.31bcd	3.52 \pm 0.30abcd	24 \pm 7abc
	DS	2.99 \pm 0.40f	2.38 \pm 0.12cd	20 \pm 4abc
Swarna	WW	4.89 \pm 0.46abc	3.58 \pm 0.17abc	27 \pm 4ab
	DS	4.38 \pm 0.55cde	2.74 \pm 0.30cd	37 \pm 7a

reduction in S_r after azide application in all varieties (Table 3) corroborates this hypothesis and demonstrates the contribution of aquaporins to root osmotic conductivity in rice. Furthermore, after a drought period, the contribution of aquaporins to S_r was significantly increased in all varieties except in Dular. However, S_r could also be affected by substantial variation in the osmotic pressure of the xylem sap, or by other unknown mechanisms contributing to root pressure (Wegner 2014). Thus, the relative S_r inhibition by azide measured in this study may not strictly reflect the function of aquaporins in osmotic water fluxes and may be considered as an “apparent” aquaporin contribution only, which may explain the lack of correlation between S_r and L_{pr} . Regardless of these considerations, by showing an increase in the aquaporin-dependent osmotic water path under drought stress, our data support a role for root aquaporins in responding to drought stress and restoring root water fluxes upon rewatering. These observations are in line with previous observations showing a role for aquaporins under water limited conditions in tobacco (*Nicotiana tabacum*) and Arabidopsis (*Arabidopsis thaliana*; Martre *et al.* 2002; Siefritz *et al.* 2002). Altogether, our data suggest an increased role for aquaporins in the modulation of rice root osmotic water fluxes under drought stress compared with well-watered conditions.

Our pharmacological approach to aquaporin inhibition using soil-grown roots involved rewatering before the measurement and treatment with an inhibitor that would effectively access the root without being absorbed by soil particles or compounds. Azide, which induces intracellular acidosis by blocking respiration via the cytochrome pathway leading to the H^+ -dependent closure of PIPs (Tournaire-Roux *et al.* 2003; Törnroth-Horsefield *et al.* 2006; Verdoucq *et al.* 2008; Sutka *et al.* 2011), is a commonly-used aquaporin inhibitor (Zhang & Tyerman 1991; Kamaluddin & Zwiazek 2001; Tournaire-Roux *et al.* 2003; Postaire *et al.* 2010; Sutka *et al.* 2011). Because complete time-dependent reversible inhibitory effects of azide

have been observed in Arabidopsis upon stopping the treatment by washing (Tournaire-Roux *et al.* 2003; Postaire *et al.* 2010), azide is generally considered to be less toxic than mercuric chloride, another common aquaporin inhibitor. In this study, azide successfully induced significant reduction of rice L_{pr} after 30 min of application with reversible effects after 60 min (Figure S3, Table 2). However, as a respiratory inhibitor, azide also induces rapid reduction in cell metabolism and membrane depolarization (Reid *et al.* 1985). Therefore, changes in osmotic pressure gradients, especially during the S_r measurements in this study, might have caused non-specific side effects on sap exudation that could have introduced an overestimation of the contribution of PIP aquaporins.

Functional determinants of root hydraulics

For further insight into the determinants of rice root hydraulics, we looked for correlation between hydraulic traits and PIP relative transcript abundance in six selected varieties. Under well-watered conditions, S_r was generally positively correlated with the overall PIP transcript abundance, especially with *PIP2;4* and *PIP2;8* (Table S4). These results suggest a specificity of these two isoforms as major contributors to osmotic water fluxes in rice, which could be particularly limiting under drought stress or during drought recovery. The correlation analyses also revealed that the induction of *PIP2;6* was particularly important in maintaining osmotic water fluxes (Table S6). L_{pr} and its relative inhibition by azide were generally negatively correlated with PIP transcript abundance under well-watered conditions and to a lesser extent under drought stress (Fig. 3a,b and Tables S4 and S5). This surprising relationship was also observed in Arabidopsis in which L_{pr} and L_{pr_Inh} were negatively correlated with transcript abundance of *AtPIP2;6* and *AtPIP2;8* (Sutka *et al.* 2011). An increase in L_{pr} and aquaporin transcript abundance was previously observed in rice within 1 to 2 h after the beginning of the light

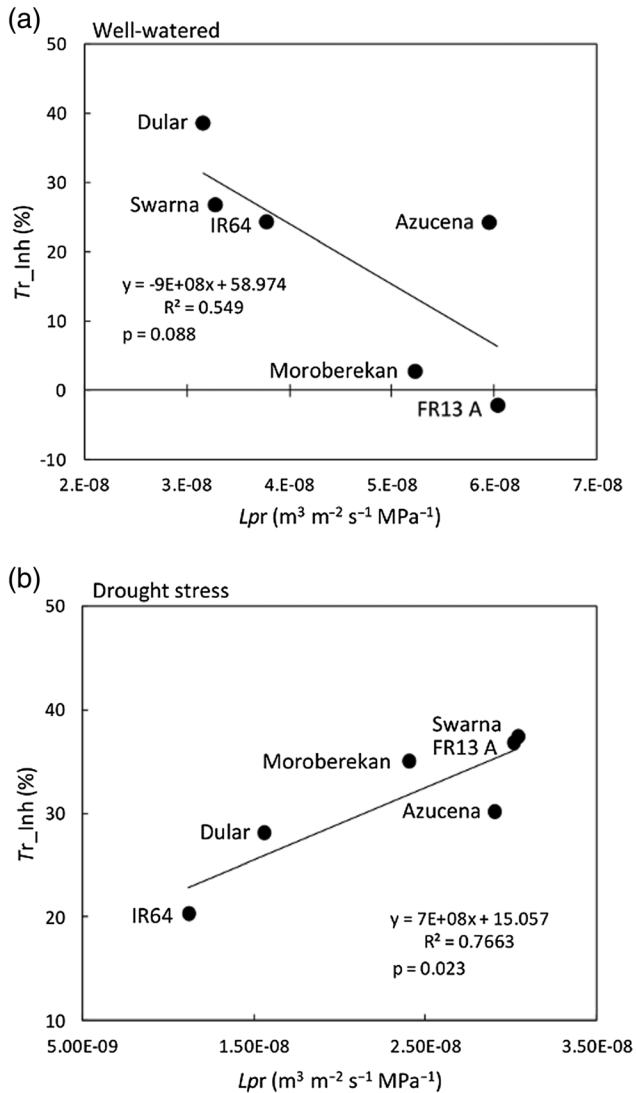


Figure 7. Correlation between Lpr and Tr_Inh in the selected varieties. Mean values of Lpr from water-treated plants and Tr_Inh by azide for each variety measured in Experiments 1 and 4, respectively, under well-watered conditions (a) or drought stress (b) are presented (see Tables 2, 5 and S12).

period, followed by a gradual decrease during the day (Sakurai-Ishikawa *et al.* 2011). Furthermore, a stronger reduction of PIP transcript abundance at mid-day was observed under drought stress compared to well-watered conditions (Henry *et al.* 2012). To limit this time of day effect, Lpr and PIP transcript abundance were measured at a specific time in this study. However, gradual PIP downregulation may explain negative correlations observed between Lpr and PIP transcript abundance, and further investigation of PIP expression over the course of the day in the 6 selected varieties under well-watered and drought stress conditions is needed. Although the physiological relevance of such relationships is still unclear, these results might also be explained by multiple post-translational modifications that can affect plant aquaporins (Li *et al.* 2014), implying that expression level and translation

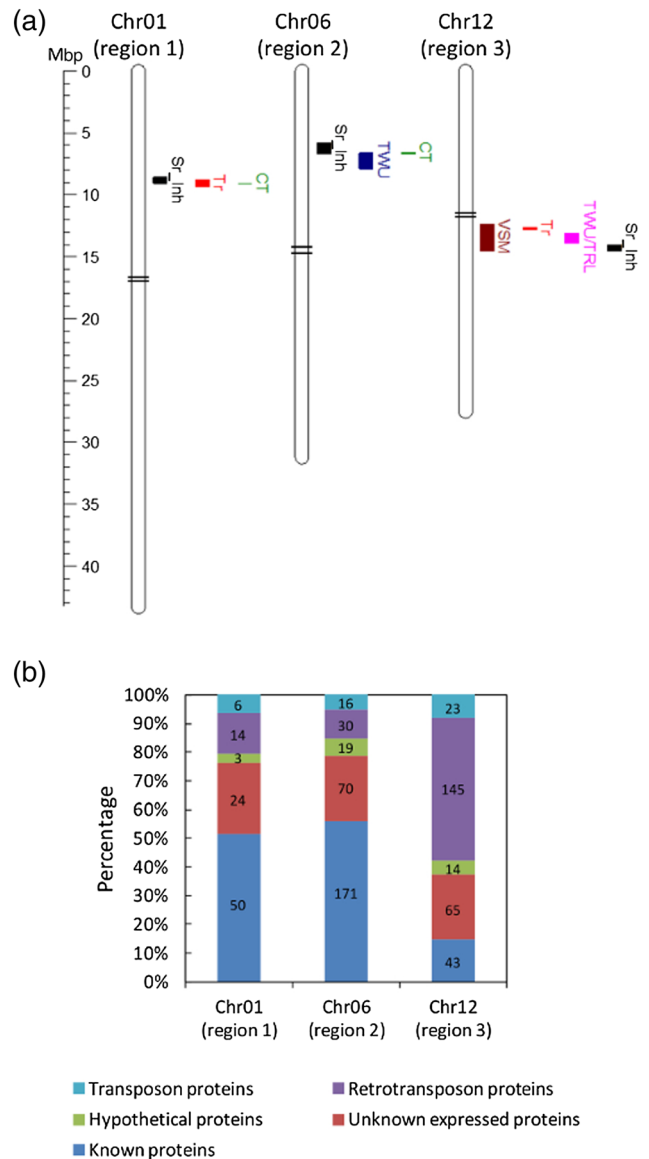


Figure 8. Chromosomal segments correlated with hydraulic and plant water use related traits. (a) Chromosome map representing genomic regions identified by introgression block regression analysis aligning for at least three different traits on chromosome 1 (Chr01), chromosome 6 (Chr06) and chromosome 12 (Chr12). Region 1 on Chr01 is located from 8.6 to 9.3 Mb and shows introgressed segments correlated with Sr_Inh (indica-type, $p = 0.00227$), Tr (indica-type, $p = 0.00237$) and CT (aus-type, $p = 0.0048$). Region 2 on Chr06 is located from 5.8 to 7.9 Mb and show introgressed segments correlated with Sr_Inh (aus-type, $p = 0.00128$), TWU (aus-type, $p = 0.00338$) and CT (aus-type, $p = 0.004$); Region 3 Chr12 is located from 12.4 to 14.5 Mb and show introgressed segments correlated with VSM (japonica-type, $p = 0.00431$), Tr (aus-type, $p = 0.0009$), TWU/TRL (aus-type, $p = 0.00032$) and Sr_Inh (aus-type, $p = 0.0039$). Sr_Inh : relative sap exudation inhibition; Tr : transpiration rate; CT: canopy temperature; TWU: total water uptake; VSM: volumetric soil moisture; TWU/TRL: total water uptake per total root length. (b) Gene content within the three regions based on percentage of genes belonging to different gene classes (based on the Nipponbare reference genome). Regions 1, 2 and 3 contain 97, 306 and 290 annotated elements respectively. The numbers of genes belonging to each class are presented on the graph.

might not be strictly related to aquaporin function. The importance of drought-induced post-translational modification of rice root aquaporins is also supported by the fact that the contribution of aquaporins to *Lpr* was differentially affected by drought in different varieties, and that no clear correlations were observed between the modulation of PIP transcript abundance and the relative aquaporin contribution to *Lpr* (i.e. *Lpr_Inh*) under drought. The concept of post-translational modification regulating aquaporin activity or localization is further supported by the identification of rice aquaporin phosphorylation sites (Whiteman *et al.* 2008; Li *et al.* 2014).

Our results showing unchanged or decreased PIP transcript abundance by drought depending on the variety is somewhat different to what was reported previously in hydroponics using PEG (Guo *et al.* 2006; Lian *et al.* 2006), and might be explained by the time of sampling, the growth conditions and the severity of the stress applied. Interestingly, we observed that the transcript abundance of certain PIPs was strongly correlated with the transcript abundance of others (Tables S4 and S5), and that some PIPs showed significant co-variation in response to drought (Table S6). This behaviour might reflect co-functionalities among aquaporins for heterotetramer formation, for instance (Fetter *et al.* 2004; Zelazny *et al.* 2007).

Structural determinants of root hydraulics

Aerenchyma formation in rice is not limited to hypoxic conditions and is also observed under aerated conditions (Jackson & Armstrong 1999). Our data obtained in soil conditions, in which a higher level of aerenchyma formation was observed in dry soil compared to well-watered conditions at 1.5 cm but not at 5 cm from the root apex, likely reflects differences in root growth rate between the well-watered and drought stress treatments. Therefore, better growth in the well-watered treatment may not yet have resulted in aerenchyma formation at the same distance from the apex as in the drought stress treatment. A positive correlation between *Lpr* and the percentage of root cortical aerenchyma was observed under well-watered conditions at 1.5 cm from the root apex but not at 5 cm or under drought stress (Tables 4, and S8–S11). Hypoxia is known to induce an acidification of root cell cytoplasm which induces the blockage of PIPs that can account for a reduction in *Lpr* (Tournaire-Roux *et al.* 2003). Although aerenchyma are typically assumed to reduce radial water flow, aerenchyma formation in the region close to the root apex, by maintaining root oxygenation, might indirectly contribute to maintaining *Lpr* by reducing cytoplasm acidification and PIP inhibition, particularly under flooded conditions. Aerenchyma could therefore have dual roles in root water fluxes, to which further investigation is needed. These results may also suggest variable water fluxes along the root axis, highlighting the importance of regions close to the root apex for water uptake. In addition to this, the observation that *Sr* was significantly positively correlated with *SD* and *MD*,

particularly under well-watered conditions (Tables S8–S10), supports the idea that root anatomical properties affect rice root hydraulics.

Root–shoot hydraulic interactions for drought tolerance

The role of aquaporins in hydraulic interactions between roots and shoots has been emphasized in several species (Maurel *et al.* 2010). For instance, modulation of maize *Lpr* using aquaporin inhibitors induced a decrease in cell turgor in the leaf elongation zone followed by a decrease in the leaf elongation rate (Ehlert *et al.* 2009). We observed that in drought-stressed plants, unlike those treated with azide, plants treated with water showed partial to complete LWP recovery (Fig. 6), suggesting that root water fluxes mediated by aquaporins play an important role in root–shoot water fluxes for LWP recovery after drought stress. This hypothesis is supported by a positive, although not significant, correlation between LWP recovery and *Sr* under drought stress ($p=0.0937$; Table S12). A similar role of root aquaporins has been suggested in transgenic lowland rice overexpressing *RWC3 (PIP1;3)*, which exhibited higher root osmotic hydraulic conductivity, LWP and cumulative transpiration after a period of 10 h of PEG treatment (Lian *et al.* 2004). Here, we observed that *Tr* recovery was more dependent on aquaporin function after drought stress than under well-watered conditions (Table 5). We also observed that *Tr* was significantly positively correlated with *Tr_Inh* (Table S12), and plants showing an activation of *Tr* by azide generally showed low *Tr*. These results suggest an isohydric-type behaviour in rice varieties with activated *Tr* that was eliminated after azide application, indicating linkages between rice plant water-balance strategies and aquaporin function in roots. Therefore the down-regulation of aquaporins may even contribute to drought tolerance in some varieties by allowing the plant to adopt a conservative strategy to maintain water fluxes and transpiration during drought stress.

Manipulating plant aquaporins in order to increase crop yield under irrigated and drought stress conditions has been addressed in several studies but with no major progress, and a better molecular understanding of the role of specific PIPs and how the plants regulate their water balance and water use efficiency, especially under drought stress conditions, is still needed (Moshelion *et al.* 2014). In this study for instance, it does not appear clearly that drought tolerance in rice is associated with high *Lpr* and *Sr*. Indeed, Azucena and Moroberekan (mildly drought tolerant), but also FR13 A and Swarna (drought susceptible) showed highest *Lpr* and *Sr* under drought stress, suggesting that other functional properties could be more related to grain yield under drought. Only in tomato (*Solanum lycopersicum*), the overexpression of a tonoplast aquaporin (*SlTIP2;2*) induced higher transpiration and significant increase in plant yield, harvest index and plant mass relative to the non-transgenic plants under well-watered and drought conditions (Sade *et al.* 2009). Because the OryzaSNP panel is a small set of genotypes that provides possibilities for testing genetic correlations with

phenotypic components, it is a very useful tool to relate functional traits that are relatively complex to measure with genomic regions by introgression block regression analysis (Jahn *et al.* 2011; Wade *et al.* 2015). Here, three genomic segments showing correlation with both root water uptake (Sr_Inh, TWU, TWU/TRL and VSM) and shoot performance (Tr and CT) were identified (Fig. 8a), which support our observations of the hydraulic interactions between roots and shoots. These segments are mostly from aus-type introgressions, which is a subgroup with characteristically more drought tolerance compared to indica- and japonica-type varieties (Glaszmann 1987). Although our study provides evidence that aquaporins are key determinants of root water fluxes in rice, no aquaporins with known water transport activity were identified in these regions (based on the Nipponbare reference genome). The absence of co-location of aquaporin genes likely reflects the complexity of root water fluxes. Modulation of water uptake to sustain shoot function under drought requires coordination of processes that are likely under the control of aquaporin-regulatory genes. Regions 1 and 2 in particular contain a number of stress-related genes such as zinc-finger proteins that could be involved (Sugano *et al.* 2003; Mukhopadhyay *et al.* 2004; Maruyama *et al.* 2012; Jan *et al.* 2013). In addition to being influenced by aquaporin expression, localization, or activity, root hydraulics also appear to depend on environmental and plant characteristics, including soil moisture, root anatomy, osmotic gradients and leaf water status.

CONCLUSIONS

Root water fluxes in rice, as in many species, were not observed to be strictly determined by the function of aquaporins, but we observed that the physiological role of these proteins became more important under drought stress. Our results suggest that rice root aquaporins can contribute but are not limiting to hydrostatic water fluxes when transpiration is high, and that they play a major role in osmotic water fluxes occurring when transpiration is low. Differences in root water fluxes were related to differences in aquaporin function, particularly for some PIP isoforms. The large genetic diversity observed among rice varieties for aquaporin expression, hydraulic properties and root anatomy, as well as the three genetic regions correlated with multiple hydraulic traits that have been identified, indicate the potential for improvement of rice water fluxes under drought. More research is necessary to pinpoint specifically how modulation of root water fluxes should be improved in order to increase the drought tolerance of rice.

ACKNOWLEDGEMENTS

This work was funded by the Generation Challenge Programme project G3008.06 'Targeting Drought-Avoidance Root Traits to Enhance Rice Productivity under Water-Limited Environments'. We thank D. Morales, L. Satioquia, A. Reyes, E. Mateo, P. Zambrano, A. Oxina, A. Los Años, E. Mico, M. Natividad, N. Sadiasa, M. Quintana, N. Turingan, C. L. Cabral and R. Torres from the IRRI Drought physiology group for technical support. At IRRI, we are also grateful to

Dr. I. H. Slamet-Loedin, Dr. N. Tsakirpaloglou and Dr. K. R. Trijatmiko for their support and advice on the RT-PCR experiment, to J. Detras for support with the Map Chart software, to V. Juanillas for support on IRRI-GSL-Galaxy analysis, to V. Bartolome for statistical support and to Dr. A. Ismail for helpful comments on the manuscript. At ICRISAT, we thank Dr. J. Kholova, S. Mallayee and M. Anjaiah for useful discussions and help in transpiration measurements, and A. C. Pandey for assistance in plant culture.

REFERENCES

- Abramoff M.D., Magalhaes P.J. & Ram S.J. (2004) Image processing with ImageJ. *Biophotonics International* **11**, 36–42.
- Ahmed A., Murai-Hatano M., Ishikawa-Sakurai J., Hayashi H., Kawamura Y. & Uemura M. (2012) Cold stress-induced acclimation in rice is mediated by root-specific aquaporins. *Plant & Cell Physiology* **53**, 1445–1456.
- Bidinger F., Mahalakshmi V. & Rao G. (1987) Assessment of drought resistance in pearl millet (*Pennisetum americanum* (L.) Leeke). II. Estimation of genotype response to stress. *Australian Journal of Agricultural Research* **38**, 49–59.
- Ehlert C., Maurel C., Tardieu F. & Simonneau T. (2009) Aquaporin-mediated reduction in maize root hydraulic conductivity impacts cell turgor and leaf elongation even without changing transpiration. *Plant Physiology* **150**, 1093–1104.
- Fetter K., Van Wilder V., Moshelion M. & Chaumont F. (2004) Interactions between plasma membrane aquaporins modulate their water channel activity. *The Plant Cell* **16**, 215–228.
- Fiscus E.L. (1986) Diurnal changes in volume and solute transport coefficients of phaseolus roots. *Plant Physiology* **80**, 752–759.
- Glaszmann J.C. (1987) Isozymes and classification of Asian rice varieties. *Theoretical and Applied Genetics* **74**, 21–30.
- Gowda V.R.P., Henry A., Vadez V., Shashidhar H.E. & Serraj R. (2012) Water uptake dynamics under progressive drought stress in diverse accessions of the OryzaSNP panel of rice (*Oryza sativa*). *Functional Plant Biology* **39**, 402–411.
- Gowda V.R.P., Henry A., Yamauchi A., Shashidhar H.E. & Serraj R. (2011) Root biology and genetic improvement for drought avoidance in rice. *Field Crops Research* **122**, 1–13.
- Guo L., Wang Z.Y., Lin H., Cui W.E., Chen J., Liu M., ... Gu H. (2006) Expression and functional analysis of the rice plasma-membrane intrinsic protein gene family. *Cell Research* **16**, 277–286.
- Henry A., Cal A.J., Batoto T.C., Torres R.O. & Serraj R. (2012) Root attributes affecting water uptake of rice (*Oryza sativa*) under drought. *Journal of Experimental Botany* **63**, 4751–4763.
- Henry A., Gowda V.R.P., Torres R.O., McNally K.L. & Serraj R. (2011) Variation in root system architecture and drought response in rice (*Oryza sativa*): phenotyping of the OryzaSNP panel in rainfed lowland fields. *Field Crops Research* **120**, 205–214.
- Jackson M.B. & Armstrong W. (1999) Formation of aerenchyma and the processes of plant ventilation in relation to soil flooding and submergence. *Plant Biology* **1**, 274–287.
- Jahn C.E., Mckay J.K., Mauleon R., Stephens J., McNally K.L., Bush D.R., ... Leach J.E. (2011) Genetic variation in biomass traits among 20 diverse rice varieties. *Plant Physiology* **155**, 157–168.
- Jan A., Maruyama K., Todaka D., Kidokoro S., Abo M., Yoshimura E., ... Yamaguchi-Shinozaki K. (2013) OsTZF1, a CCCH-tandem zinc finger protein, confers delayed senescence and stress tolerance in rice by regulating stress-related genes. *Plant Physiology* **161**, 1202–1216.
- Javot H. & Maurel C. (2002) The role of aquaporins in root water uptake. *Annals of Botany* **90**, 301–313.
- Kamaluddin M. & Zwiazek J.J. (2001) Metabolic inhibition of root water flow in red-osier dogwood (*Cornus stolonifera*) seedlings. *Journal of Experimental Botany* **52**, 739–745.
- Kamoshita A., Wade L.J. & Yamauchi A. (2000) Genotypic variation in response of rainfed lowland rice to drought and rewatering. III. Water extraction during the drought period. *Plant Production Science* **3**, 189–196.
- Katsuhara M., Koshio K., Shibasaki M., Hayashi Y., Hayakawa T. & Kasamo K. (2003) Over-expression of a barley aquaporin increased the shoot/root ratio and raised salt sensitivity in transgenic rice plants. *Plant & Cell Physiology* **44**, 1378–1383.

- Kawahara Y., Bastide M.D., Hamilton J.P., Kanamori H., McCombie W.R., Ouyang S., ... Matsumoto T. (2013) Improvement of the *Oryza sativa* Nipponbare reference genome using next generation sequence and optical map data. *Rice* **6**, 1–10.
- Kholová J., Hash C.T., Kumar P.L., Yadav R.S., Kocová M. & Vadez V. (2010) Terminal drought-tolerant pearl millet [*Pennisetum glaucum* (L.) R. Br.] have high leaf ABA and limit transpiration at high vapour pressure deficit. *Journal of Experimental Botany* **61**, 1431–1440.
- Kondo M., Murty M.V.R. & Aragones D.V. (2000) Characteristics of root growth and water uptake from soil in upland rice and maize under water stress. *Soil Science and Plant Nutrition* **46**, 721–732.
- Li G.-W., Peng Y.H., Yu X., Zhang M.H., Cai W.M., Sun W.N., ... Su W.A. (2008) Transport functions and expression analysis of vacuolar membrane aquaporins in response to various stresses in rice. *Journal of Plant Physiology* **165**, 1879–1888.
- Li G., Santoni V. & Maurel C. (2014) Plant aquaporins: roles in plant physiology. *Biochimica et Biophysica Acta* **1840**, 1574–1582.
- Lian H.L., Yu X., Lane D., Sun W.N., Tang Z.C. & Su W.A. (2006) Upland rice and lowland rice exhibited different PIP expression under water deficit and ABA treatment. *Cell Research* **16**, 651–660.
- Lian H.L., Yu X., Ye Q., Ding X., Kitagawa Y., Kwak S.O., ... Ding X.S. (2004) The role of aquaporin RWC3 in drought avoidance in rice. *Plant & Cell Physiology* **45**, 481–489.
- Liu C., Fukumoto T., Matsumoto T., Gena P., Frascaria D., Kanedo T., ... Kitagawa Y. (2013) Aquaporin OsPIP1:1 promotes rice salt resistance and seed germination. *Plant Physiology and Biochemistry* **63**, 151–158.
- Lu Z. & Neumann P.M. (1999) Water stress inhibits hydraulic conductance and leaf growth in rice seedlings but not the transport of water via mercury-sensitive water channels in the root. *Plant Physiology* **120**, 143–151.
- Lynch J.P. (2013) Steep, cheap and deep: an ideotype to optimize water and N acquisition by maize root systems. *Annals of Botany* **112**, 347–357.
- Malz S. & Sauter M. (1999) Expression of two PIP genes in rapidly growing internodes of rice is not primarily controlled by meristem activity or cell expansion. *Plant Molecular Biology* **40**, 985–995.
- Martre P., Morillon R., Barrieu F., North G.B., Nobel P.S. & Chrispeels M.J. (2002) Plasma membrane aquaporins play a significant role during recovery from water deficit. *Plant Physiology* **130**, 2101–2110.
- Maruyama K., Todaka D., Mizoi J., Yoshida T., Kidokoro S., Matsukura S., ... Yamaguchi-Shinozaki K. (2012) Identification of cis-acting promoter elements in cold- and dehydration-induced transcriptional pathways in Arabidopsis, rice, and soybean. *DNA Research* **19**, 37–49.
- Matsuo N., Ozawa K. & Mochizuki T. (2009) Genotypic differences in root hydraulic conductance of rice (*Oryza sativa* L.) in response to water regimes. *Plant and Soil* **316**, 25–34.
- Maurel C., Simonneau T. & Sutka M. (2010) The significance of roots as hydraulic rheostats. *Journal of Experimental Botany* **61**, 3191–3198.
- McNally K.L., Childs K.L., Bohnert R., Davidson R.M., Zhao K., Ulat V.J., ... Leach J.E. (2009) Genomewide SNP variation reveals relationships among landraces and modern varieties of rice. *Proceedings of the National Academy of Sciences of the United States of America* **106**, 12273–12278.
- Miyamoto N., Steudle E., Hirasawa T. & Lafitte R. (2001) Hydraulic conductivity of rice roots. *Journal of Experimental Botany* **52**, 1835–1846.
- Morita S. & Abe J. (2002) Diurnal and phenological changes of bleeding rate in lowland rice plants. *Japanese Journal of Crop Science* **71**, 383–388.
- Moshelion M., Halperin O., Wallach R., Oren R. & Way D. (2014) Role of aquaporins in determining transpiration and photosynthesis in water-stressed plants: crop water-use efficiency, growth and yield. *Plant, Cell & Environment* doi: 10.1111/pce.12410.
- Mukhopadhyay A., Vij S. & Tyagi A.K. (2004) Overexpression of a zinc-finger protein gene from rice confers tolerance to cold, dehydration, and salt stress in transgenic tobacco. *Proceedings of the National Academy of Sciences of the United States of America* **101**, 6309–6314.
- Nada R.M. & Abogadallah G.M. (2014) Aquaporins are major determinants of water use efficiency of rice plants in the field. *Plant Science: an International Journal of Experimental Plant Biology* **227**, 165–180.
- Nguyen M.X., Moon S. & Jung K.-H. (2013) Genome-wide expression analysis of rice aquaporin genes and development of a functional gene network mediated by aquaporin expression in roots. *Planta* **238**, 669–681.
- Ouyang S., Zhu W., Hamilton J., Lin H., Campbell M., Childs K., ... Buell C.R. (2007) The TIGR rice genome annotation resource: improvements and new features. *Nucleic Acids Research* **35**, D883–D887.
- Postaire O., Tournaire-Roux C., Grondin A., Boursiac Y., Morillon R., Schäffner A.R., ... Maurel C. (2010) A PIP1 aquaporin contributes to hydrostatic pressure-induced water transport in both the root and rosette of Arabidopsis. *Plant Physiology* **152**, 1418–1430.
- Ranathunge K., Kotula L., Steudle E. & Lafitte R. (2004) Water permeability and reflection coefficient of the outer part of young rice roots are differently affected by closure of water channels (aquaporins) or blockage of apoplastic pores. *Journal of Experimental Botany* **55**, 433–447.
- Ranathunge K., Steudle E. & Lafitte R. (2003) Control of water uptake by rice (*Oryza sativa* L.): role of the outer part of the root. *Planta* **217**, 193–205.
- Reid R.J., Dejaegere R. & Pitman M.G. (1985) Regulation of electrogenic pumping in barley by pH and ATP. *Journal of Experimental Botany* **36**, 535–549.
- Rogers E.D. & Benfey P.N. (2015) Regulation of plant root system architecture: implications for crop advancement. *Current Opinion in Biotechnology* **32**, 93–98.
- Sade N., Vinocur B.J., Diber A., Shatil A., Ronen G., Nissan H., ... Moshelion M. (2009) Improving plant stress tolerance and yield production: is the tonoplast aquaporin *S7TIP2;2* a key to isohydric to anisohydric conversion? *New Phytologist* **181**, 651–661.
- Sakurai-Ishikawa J., Murai-Hatano M., Hayashi H., Ahamed A., Fukushi K., Matsumoto T. & Kitagawa Y. (2011) Transpiration from shoots triggers diurnal changes in root aquaporin expression. *Plant, Cell & Environment* **34**, 1150–1163.
- Sakurai J., Ahamed A., Murai M., Maeshima M. & Uemura M. (2008) Tissue and cell-specific localization of rice aquaporins and their water transport activities. *Plant & Cell Physiology* **49**, 30–39.
- Sakurai J., Ishikawa F., Yamaguchi T., Uemura M. & Maeshima M. (2005) Identification of 33 rice aquaporin genes and analysis of their expression and function. *Plant & Cell Physiology* **46**, 1568–1577.
- Siefritz F., Tyree M.T., Lovisolo C., Schubert A. & Kaldenhoff R. (2002) PIP1 plasma membrane aquaporins in tobacco: from cellular effects to function in plants. *The Plant Cell* **14**, 869–876.
- Steudle E. (2000) Water uptake by roots: effects of water deficit. *Journal of Experimental Botany* **51**, 1531–1542.
- Sugano S., Kaminaka H., Rybka Z., Catala R., Salinas J., Matsui K., ... Takatsui H. (2003) Stress-responsive zinc finger gene *ZPT2-3* plays a role in drought tolerance in petunia. *The Plant Journal* **36**, 830–841.
- Sutka M., Li G., Boudet J., Boursiac Y., Doumas P. & Maurel C. (2011) Natural variation of root hydraulics in Arabidopsis grown in normal and salt-stressed conditions. *Plant Physiology* **155**, 1264–1276.
- Törnroth-Horsefield S., Wang Y., Hedfalk K., Johanson U., Karlsson M., Tajkhorshid E., ... Kjellbom P. (2006) Structural mechanism of plant aquaporin gating. *Nature* **439**, 688–694.
- Tournaire-Roux C., Sutka M., Javot H., Gout E., Gerbeau P., Luu D.T., ... Maurel C. (2003) Cytosolic pH regulates root water transport during anoxic stress through gating of aquaporins. *Nature* **425**, 393–397.
- Vadez V. (2014) Root hydraulics: the forgotten side of roots in drought adaptation. *Field Crops Research* **165**, 15–24.
- Verdoucq L., Grondin A. & Maurel C. (2008) Structure–function analysis of plant aquaporin AtPIP2;1 gating by divalent cations and protons. *The Biochemical Journal* **415**, 409–416.
- Voorrips R.E. (2002) MapChart: software for the graphical presentation of linkage maps and QTLs. *The Journal of Heredity* **93**, 77–78.
- Wade L., Bartolome V., Mauleon R., Vasant V., Prabakar S., Chelliah M., ... Henry A. (2015) Environmental response and genomic regions correlated with rice root growth and yield under drought in the OryzaSNP panel across multiple study systems. *PLoS One* doi: 10.1371/journal.pone.0124127.
- Wegner L.H. (2014) Root pressure and beyond: energetically uphill water transport into xylem vessels? *Journal of Experimental Botany* **65**, 381–393.
- Whiteman S.A., Nühse T.S., Ashford D., Sanders D. & Maathuis F.J.M. (2008) A proteomic and phosphoproteomic analysis of *Oryza sativa* plasma membrane and vacuolar membrane. *The Plant Journal* **56**, 146–156.
- Zelazny E., Borst J.W., Muylaert M., Batoko H., Hemming M.A. & Chaumont F. (2007) FRET imaging in living maize cells reveals that plasma membrane aquaporins interact to regulate their subcellular localization. *Proceedings of the National Academy of Sciences of the United States of America* **104**, 12359–12364.
- Zhang W.H. & Tyerman S.D. (1991) Effect of low O₂ concentration and azide on hydraulic conductivity and osmotic volume of the cortical cells of wheat roots. *Functional Plant Biology* **18**, 603–613.
- Zimmermann H.M., Hartmann K., Schreiber L. & Steudle E. (2000) Chemical composition of apoplastic transport barriers in relation to radial hydraulic conductivity of corn roots (*Zea mays* L.). *Planta* **210**, 302–311.

Received 23 April 2015; accepted for publication 26 July 2015

SUPPORTING INFORMATION

Additional Supporting Information may be found in the online version of this article at the publisher's web-site:

Table S1. Characteristics of the soil used for the experiments in this study, as analyzed by the Analytical Service Laboratory (ASL) at IRRI. Soil characteristics were not available for Experiment 6.

Table S2. Conditions in the growth chamber at the time of transpiration rate measurements. The pots were weighed every hour from 8 AM to 4 PM while the VPD conditions were increasing inside the growth chamber.

Table S3. Table of primers used for RT-PCR. Primer sequences were derived from Sakurai et al. (2005).

Table S4. Correlation between root PIP transcript abundance, root hydraulic properties (Lpr, Sr) and root hydraulic inhibition by azide (Lpr_Inh and Sr_Inh) under well-watered conditions (WW) in six selected rice varieties. Values indicate the Pearson's coefficient of correlation. *: p-values < 0.05; **: p-values < 0.01.

Table S5. Correlation between root PIP transcript abundance, root hydraulic properties (Lpr, Sr) and root hydraulic inhibition by azide (Lpr_Inh and Sr_Inh) under drought stress conditions (DS) in six selected rice varieties. Values indicate the Pearson's coefficient of correlation. *: p-values < 0.05; **: p-values < 0.01.

Table S6. Correlation between root PIP transcript variation under drought, root hydraulic properties (Lpr, Sr) and root hydraulic inhibition by azide (Lpr_Inh and Sr_Inh) under drought stress conditions in six selected rice varieties. Values indicate the Pearson's coefficient of correlation. *: p-values < 0.05; **: p-values < 0.01. ***: p-values < 0.05.

Table S7. Root morphology of six selected rice varieties. Roots of plants grown under well-watered conditions (WW) or drought stress (DS) in Experiment 1 (\$) and Experiment 2 (*) were sampled and washed to remove soil residues at 29 and 35 das, respectively. Mean values \pm se of $n=29-30$ and $n=8-12$ biological replications are presented. Letters indicate different significant groups in WW or DS soil moisture treatment. No significant differences were observed among varieties for root mass or root:shoot ratio.

Table S8. Correlation between root anatomical traits at 1.5 cm from the root apex, root hydraulic properties (Lpr, Sr) and root hydraulic inhibition by azide (Lpr_Inh and Sr_Inh) under well-watered conditions (WW) in six selected rice varieties. RD: root diameter; CCD: cortex cell diameter; Ae: percent cortical aerenchyma; SD: stele diameter; MD: metaxylem diameter. Values indicate the Pearson's coefficient of correlation.

Table S9. Correlation between root anatomical traits at 1.5 cm from the root apex, root hydraulic properties (Lpr, Sr) and root hydraulic inhibition by azide (Lpr_Inh and Sr_Inh) under well-watered conditions (WW) in six selected rice varieties. RD: root diameter; CCD: cortex cell diameter; Ae: percent cortical aerenchyma; SD: stele diameter; MD: metaxylem diameter. Values indicate the Pearson's coefficient of correlation.

Table S10. Correlation between root anatomical traits at 1.5 cm from the root apex, root hydraulic properties (Lpr, Sr) and root

hydraulic inhibition by azide (Lpr_Inh and Sr_Inh) under well-watered conditions (WW) in six selected rice varieties. RD: root diameter; CCD: cortex cell diameter; Ae: percent cortical aerenchyma; SD: stele diameter; MD: metaxylem diameter. Values indicate the Pearson's coefficient of correlation.

Table S11. Correlation between root anatomical traits at 5 cm from the root apex, root hydraulic properties (Lpr, Sr) and root hydraulic inhibition by azide (Lpr_Inh and Sr_Inh) under drought-stress conditions (DS) in six selected rice varieties. RD: root diameter; CCD: cortex cell diameter; Ae: percent cortical aerenchyma; SD: stele diameter; MD: metaxylem diameter. Values indicate the Pearson's coefficient of correlation. *: p-values < 0.05; **: p-values < 0.01.

Table S12. Correlations among root hydraulic properties (Lpr, Sr), root hydraulic inhibition by azide (Lpr_Inh and Sr_Inh), leaf transpiration (Tr), inhibition of transpiration by azide (Tr_Inh) and leaf water potential (LWP) under well-watered conditions and drought stress in six selected rice varieties. LprW, LprW_Inh, SrW, SrW_Inh, TrW, TrW_Inh and LWPW were measured from water-treated plants grown under well-watered conditions. LprD, LprD_Inh, SrD, SrD_Inh, TrD, TrD_Inh and LWPD were measured from water-treated plants grown under drought stress. Values indicate the Pearson's coefficient of correlation. *: p-values < 0.05; **: p-values < 0.01.

Table S13. Data set used for the identification of introgressed chromosome segments correlated with hydraulic and drought tolerance related traits presented in Figure 8. Sr, Sr_inh: Sr and relative Sr inhibition by azide were measured on plants grown under well-watered conditions in Experiment 5. Tr, Tr_inh: cumulative water loss by transpiration 2 hours after rewatering the plants with water normalized by the leaf area, and relative Tr inhibition by azide were measured in Experiment 6; TWU, TWU/TRL: total water uptake and total water uptake per total root length data are from Gowda et al. (2012). VSM: volumetric soil moisture data are from Henry et al. (2011); Sr_DS: Sr normalized by the shoot dry weight measured under drought stress is from Experiment 7 at 82 das. CT: canopy temperature measured under drought stress is from Experiment 7 at 81 das. SDW reduction: reduction in shoot dry weight measured under drought stress compared to shoot dry weight measured under well-watered conditions at maturity (117 das) is from Experiment 7. DRI: drought response index was measured in Experiment 7.

Figure S1. Soil water potential readings during the field experiment. Tensiometers were installed at a depth of 30 cm in Experiment 7. Soil was rewatered at 95 das. Mean values \pm se of $n=3$ tensiometer readings are presented.

Figure S2. Environmental characteristics during Experiment 7. The field experiment was performed during the dry season 2014 at the IRRI farm, Los Baños, Philippines (14° 11'N, 121° 15'E). Weather data are from the IRRI Climate Unit.

Figure S3. Optimization of the Lpr inhibition measurement protocol using aquaporin inhibitors. Plants were grown in soil-filled mylar tubes for 29 days under well-watered conditions. (A) Roots were washed to remove soil compounds and placed into water, salt (500 mM; left panel) or azide solution

(4 mM; right panel). (B) Soil was directly rewatered with 150 ml of water, salt (500 mM; left panel) or azide solution (4 mM; right panel). *Lpr* was measured by collecting exuded xylem sap flux after pressurizing the roots after 30 or 60 minutes of water or inhibitor treatments. Bars show mean values \pm se of $n=2-5$ plants. *: p -values < 0.05 .

Figure S4. Effect of time of day on *Lpr* and relative *Lpr* inhibition (*Lpr_Inh*) by azide under well-watered and drought stress conditions. *Lpr* from water-treated plants (A, B) and *Lpr_Inh* (C, D) were measured in Experiment 1 from 7:30 AM to 10:00 AM (early) and from 10:00 AM to 1:00 PM (mid) under well-watered (A, C) and drought stress conditions (B, D). Bars show mean \pm se of $n=3-10$ plants. *: p -values < 0.05 ; **: p -values < 0.01 .

Figure S5. Visualization of plasma membrane aquaporin (PIP) amplicons after RT-PCR. cDNA was prepared from roots grown in Experiment 3 under well-watered and drought stress conditions. 20 μ L of RT-PCR products of PIP1;1 (A), PIP1;2 (B), PIP1;3 (C), PIP2;1 (D), PIP2;2 (E), PIP2;4 (F), PIP2;6

(G) and PIP2;8 (H) together with products of ubiquitin from the three biological replicates per variety amplified in the same RT-PCR run were stained using SYBR® safe DNA (Invitrogen, California, USA) and subjected to agarose gel electrophoresis. The signal intensity of the bands was observed by an Infinity ST5 v16.08a imaging system (Vilber Lourmat, France).

Figure S6. Root anatomy of Azucena, Moroberekan, FR13 A, Dular, IR64 and Swarna. Representative images from cross sections of nodal roots at 5 cm from the root apex of plants grown under well-watered conditions (A, C, E, G, I and K) and drought stress (B, D, F, H, J and L) in Experiment 1 are shown. The bar represents 400 μ m.

Figure S7. Correlation of Sr and Tr with their respective level of inhibition by azide under well-watered conditions in the OryzaSNP panel. Positive correlation between Sr and Sr_Inh (A) and between Tr and Tr_Inh (B) were observed under well-watered conditions in Experiments 5 and 6, respectively (see Table S12).